Effects of Staircases on Seismic Performance of RC Buildings

Abdelhakim Alhussein

Submitted to the
Institute of Graduate Studies and Research
in partial fulfillment of the requirements for the degree of

Master of Science
in
Civil Engineering

Eastern Mediterranean University
January 2019
Gazimağusa, North Cyprus

Approval of the Institute of Graduate Studies and Research

Assoc. Prof. Dr. Ali Hakan Ulusoy
Acting Director

I certify that this thesis satisfies all the requirements as a thesis for the degree of Master of Science in Civil Engineering.

Assoc. Prof. Dr. Serhan Şensoy
Chair, Department of Civil Engineering

We certify that we have read this thesis and that in our opinion it is fully adequate in scope and quality as a thesis for the degree of Master of Science in Civil Engineering.

Assoc. Prof. Dr. Mehmet Cemal Geneş
Supervisor

Examining Committee

1. Assoc. Prof. Dr. Mehmet Cemal Geneş

2. Assoc. Prof. Dr. Rifat Reşatoğlu

3. Asst. Prof. Dr. Umut Yıldırım

ABSTRACT

In recent years, the design for seismic resistance has been undergone a critical reassessment with the emphasis of altering from strength to performance. The recent earthquakes in some parts of the world have exposed a catastrophic impact on civil areas. Turkey has been hit by several moderate to large earthquakes over the last decades, which have led to significant loss of life and property, the extreme damage and building collapse has indicated to insufficient seismic behaviour of multi-storey reinforced concrete buildings. Staircases are the main emergency exist in buildings and they are significantly important for escaping after earthquake, damages have been experienced in structures during earthquake because of the interaction of staircase and structure elements. This study investigates the impact of staircase and its location on the seismic performance of reinforced concrete building. Eight structures have been modelled by ETABS 16 program, four of them with considering staircase in four locations and four without considering staircase. Linear Static, Non-linear Static Push over and Non-linear Time History analysis methods have been conducted by utilizing ETABS 16 program to evaluate the staircase effect on seismic performance of reinforced concrete buildings. It was observed that the staircase presence and its location affect the steel reinforcement ratio of columns, displacements, base shear force, stiffness, formation of short columns and formation of plastic hinges.

Keywords: seismic performance, reinforced concrete buildings, staircases, push over analysis, time History analysis.

ÖZ

Son yıllarda, yapıların sismik etkilere karşı tasarımı, dayanımdan performansa değişim vurgusuyla yeni kritik bir değerlendirmeden geçirilmiştir. Dünyanın bazı bölgelerinde son zamanlarda meydana gelen depremler sivil alanlar üzerinde yıkıcı bir etki yaratmıştır. Türkiye, son 20-30 yılda önemli ölçüde can ve mal kaybına neden olan birkaç büyük ve orta şiddetli depremden etkilenmiştir. Gözlenen aşırı hasar ve bina çökmeleri, çok katlı betonarme yapıların yetersiz sismik davranışına işaret etmiştir. Merdivenler, binalarda var olan ve hayati önem taşıyan, acil durumlarda ve depremden sonra kaçmak için çok önemli yapı elemanlarıdır. Merdiven ve yapı elemanlarının etkileşimi nedeniyle deprem sırasında yapılarda hasar meydana geldiği gözlemlenmiştir. Bu çalışmada, merdivenin ve bulunduğu yerin, betonarme yapının sismik performansı üzerindeki etkisi araştırılmıştır. Sekiz yapı ETABS 16 programı ile, dördü farklı dört yerde merdiven düşünülerek, ve diğer dördü de merdiven düşünülmeden modellenmiştir. Merdivenlerin betonarme yapıların sismik performansı üzerindeki etkisini değerlendirmek için Doğrusal Statik, Doğrusal Olmayan Statik İtme ve Doğrusal Olmayan Zaman Tanım Alanında analiz yöntemleri kullanılarak ETABS 16 programı ile analizler yapılmıştır. Merdiven mevcudiyetinin ve bulunduğu yerin, kolon donatı oranını, yer değiştirmeleri, taban kesme kuvvetini, rijitliği ve plastik mafsal oluşumunu etkilediği gözlenmiştir.

Anahtar Kelimeler: Sismik performans, betonarme binalar, merdivenler, push over analizi, time History analizi.

ACKNOWLEDGMENT

I would like to thank Dr. Mehmet Cemal Geneş for his valuable suggestions and guidance, I sincerely appreciate all the time he spent on this research work. I would also like to thank to all the members of the Civil Engineering Department.

TABLE OF CONTENTS

LIST OF TABLES

LIST OF FIGURES

LIST OF SYMBOLS AND ABBREVIATIONS

$(\Delta_i)avr$	Average Relative Storey Drift
η_{bi}	Torsional Irregularity Factor
$\boldsymbol{n}$	Live Load Participation Factor
δ_t	Target Displacement
A_0	Effective Ground Acceleration Coefficient
I	Building Importance Factor
K_e	Effective Lateral Stiffness of the Structure
K_i	Elastic Lateral Stiffness of the Structure
Q_D	Dead Load
Q_L	Effective Live Load
R	Structural System Behavior Factor
S_{aR}	Reduced Acceleration Spectrum
S(T)	Spectrum Coefficient
TA, TB	Spectrum Characteristic Periods
V_t	Base Shear

Chapter 1

INTRODUCTION

1.1 General Introduction

Civil engineering structures may be affected during their lifetime by natural disasters such as earthquakes, hurricanes, tornadoes, floods, fires and man-made and artificial disasters such as explosion and impact. Generally, reinforced concrete buildings are designed in accordance with the designed codes and standards which commonly consider dead, imposed, and earthquake loads. However, the influence of staircase is usually overlooked in seismic design of frame structures.

Turkey has been hit by several moderate to large earthquakes over the last two decades, which have led to significant loss of life and property for instance, in Kocaeli earthquake 1999 the official death toll was further than 15 000, with nearly 44 000 people injured and thousands left displaced, the total of 330 000 houses were damaged. This significant number of victims and severely damaged or collapsed buildings has highlighted insufficient seismic performance of multi-storey reinforced concrete buildings, usually three to seven stories in height (Inel, Ozmen & Bilgin, 2008).

Because the modeling is easy and fast, many designers do not consider the staircases during the modeling of the building for performing analysis. But, it has been determined during the damage assessment investigations made after the moderate

and severe earthquakes that significant damages were observed in the stairs and the columns in which they were supported, although there was no serious damage to the general frame system of the buildings.

Over the past 20 years, nonlinear static analysis or pushover analysis has been developed and has become the favoured analytical procedure for design and seismic performance evaluation purposes, as the procedure is comparatively simple and considers post- elastic behaviour. Pushover analysis is an approximate analysis method in which the structure is exposed to monotonically increasing lateral forces until a target displacement is exceeded.

1.2 Research Objectives

The overall aim of this study was to evaluate the influence of the staircase and its location on the seismic performance of reinforced concrete buildings by conducting Linear Static, Non-linear Static Pushover and Time History analysis methods. In purpose of investigating the staircase and its location effect on the seismic behaviour of RC structures an eight reinforced concrete buildings were modelled and designed by ETABS 2016 software (version 16.2.1), four of these buildings were designed with considering staircase with four different locations, and the other four buildings were designed without including staircase, in other words the staircase place left empty. The results of analysis methods are compared in terms of torsional and inter-storey stiffness irregularities, reinforcement ratios, monitored displacements, spectral displacement, shear forces, stiffness, diaphragm centre mass of displacements, max drift storey and the formation of plastic hinges.

Staircases are the main vertical emergency exit routes in multi-storey buildings, which are critically important after earthquakes for exit and access. Staircase must remain serviceable after moderate or severe ground shaking, so that residents can continue to be evacuated quickly (Roha et al., 1982).

1.3 Staircase Definition and Components

Staircase provides means of movement in a structure from one floor to another. Staircases comprises of several steps with landing at appropriate intervals to afford users with comfort and safety. The staircase comprises of steps, landing slab and flight slab as displayed in Figure 1.1.

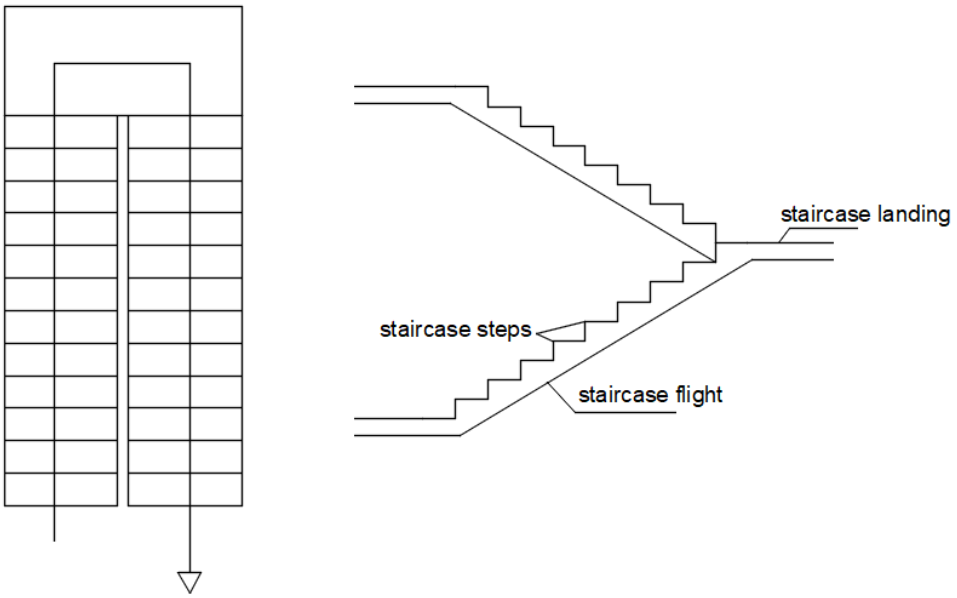

Figure 1.1: Staircase components.

Figure 1.1 shows staircase components, flight of staircase with a slope with / without treads connecting more slabs or a slab with a landing. Landing of staircase is an element that allows the flight of staircase to change direction or, in the case of very long flights, allows people to rest on the staircase.

1.4 Organization of the Thesis

Chapter one objects to provide a general introduction, research objectives of the present study and definition of staircase.

Chapter two is specialized to give information about seismic influence of concrete staircase during many earthquakes in different countries, and the past studies on the effect of concrete staircase on the seismic behaviour.

Chapter three is a methodology, it contains an explanation of buildings modelling by ETABS program, the characteristics, defining Linear Static analysis method, describing Non-linear Static Pushover analysis method and Time History analysis method.

Chapter four comprises results and discussions. In this chapter, results and discussions are divided into three main parts, first is the Static analysis method results and discussions in terms of torsional irregularity A1, Inter-storey Stiffness Irregularity (Soft Storey) B2 and steel reinforcement ratios of staircase columns. The second part discuss the Non-linear Static Pushover analysis method results and discussions in terms of plastic hinges phases, base shear forces, monitored displacements, spectral displacements, initial stiffness and effective stiffness. The third part present the discussion of Time History analysis outcomes in terms of diaphragm center of mass displacements, storey drifts and formation of plastic hinges.

Chapter five consist of conclusion and recommendations. The conclusion of the thesis is summarized for both Linear Static analysis method, Non-linear Static

Pushover and Time History analysis method, finally recommendations for future studies are proposed.

Chapter 2

LITERATURE REVIEW

2.1 Introduction

This chapter provides the background and study of literature review concerning the impact of concrete staircase and its location on the seismic behaviour of reinforced concrete buildings under lateral loads. First part discuss the description of the concrete staircase performance and its effects on the structure during earthquake. Selected past studies on the concrete staircase impact on the seismic performance of reinforced concrete building are provided in the second part.

2.2 Seismic Influence of Concrete Staircase

In multi-story buildings the primary function of the staircase is an emergency exit routes. The staircase must be designed in proper way that its function for safe exodus during and after earthquake can be guaranteed. The interaction between the staircase structural elements and primary structural system of the building is the reason of most earthquake failures and damages (Roha, Axley & Bertero, 1982).

A huge number of reinforced concrete buildings were collapsed or severely destructed throughout Zem-mouri earthquake which struck northern Algeria on May 21, 2003. An investigation was prepared to estimate damage. It is observed that there is damage in staircase columns as shown in Figure 2.1. Staircase usually divide the columns at mid story height which generates short columns. This problem is

overlooked in designing columns and as result collapse may occur (Bechtoula & Ousalem, 2005).

Figure 2.1: Staircase column damage Zem-mouri earthquake in Algeria (Bechtoula &Ousalem, 2005).

A minor to extreme damage of huge number of staircases were experienced in Wenchuan earthquake that struck the north western Sichuan on May 12, 2008. An investigation was conducted to in the epicentral region, the seismic damage of the staircases and their configurations were inspected. The interaction of staircase and the primary structure elements leads to numerous types of seismic destruction to the staircase or the primary structure elements as displayed in Figure 2.2 and 2.3, the creation of short column and beam-column connection of the staircase influenced the primary elements of the structure (Li & Mosalam, 2012).

Figure 2.2: Short column damage Wenchuan earthquake China 2008 (Li & Mosalam, 2012).

Figure 2.3: Beam-column connection damage Wenchuan earthquake China 2008 (Li & Mosalam, 2012).

Damages of buildings of the earthquake that shook Tabanlı (Van) in Turkey during October 23, 2011 were investigated, it is obtained that staircase of the structures experienced extreme damage throughout the earthquake because of the inappropriate reinforcement detailing. It was also observed that the formation of short columns can

be classified as one of the most frequently obtained deficiencies (Tapan, Comert, Demir, Sayan, Orakcal & Ilki 2013).

An earthquake struck the Gorkha District of Nepal on April 25, 2015, failures and damages were studied. It is obtained that one of the most commonly experienced damage is the creation of short column due to intermediate staircase landing in between two floors as shown in Figure 2.4 (Sharma, Deng & Noguez 2016).

Figure 2.4: Short column failures Gorkha District of Nepal on April 25, 2015 (Sharma, Deng & Noguez 2016).

2.3 Past Studies on the Staircase Impact On Seismic Performance of Structure

Base shear method, spectrum analysis and time history analysis to four models of concrete frame with staircase were conducted by using ETABS program in order to inspect the seismic performance of these models in elastic-phase. It is observed that involving staircase into models affect the seismic performance of frame structure significantly (Dai & Qi, 2009).

The seismic performance of four models that are concrete frame structure with and without staircase is studied by adopting base shear method and spectrum analysis by utilizing ETABS program. The outcomes of the analyses show that the story-stiffness distribution, shear-ratio of staircase-frame column of frame structure and vibration mode are influenced considerably in the models that involve staircase and these effects are depending on mid-platform connecting to staircase frame column or not (Dai & Qi, 2010).

Simulation of several common layout arrangements for staircase in order to create mathematical modeling in propose of investigating the staircase impact on the structure seismic performance, it is obtained that the staircase arrangement has a great influence on the displacement and internal force of the structure (Ke, Fang-cun, Ke-shuan & Jin-hua, 2011).

A building with staircase location in the center of the structure and without staircase is modelled by using SAP2000 software to analysis the structural model and make a comparison. The study results show that the stiffness of Y direction which is parallel to the staircase direction is greater than X direction which is vertical direction of staircase the columns shear force (X direction) and moment (X / Y directions) of columns increased in model that including staircase (Zheng, Liao & Zhu, 2011).

The seismic response of three models which are reinforced concrete frame structure is investigated by applying spectrum analysis and time history method on ETABS program, one of these models is with staircase the two others are with different thickness staircase mid-platform disconnecting to staircase frame column. The outcomes of the study show that the role of staircase is similar to bracing in staircase

plank direction, it is also obtained that including staircase into models affect the distribution of story stiffness, for models that have different thickness staircase mid-platform had non-considerable difference on seismic response of frame structure in two directions (Dai & Qi, 2011).

A time-history analysis of a five-floor reinforced concrete frame structure with cranked slab staircase was conducted by utilizing the finite element software Midas/Gen for model structure. The seismic responses of frame with and without stairs are compared. The results direct that staircase is a weak part, the stress in staircase is greater than that in frame and the failure of the model begins from the staircase and progresses from the lower floor to up (Jing, Zhang & Tina, 2012).

The structure design and the whole structure forces are influenced by the staircases, the frame structure forces that are close to staircases change significantly and more simply to be damaged during the earthquake, the internal force distributions can be changed by the staircase location. The frame columns internal forces are influenced by the stair flight support effects. The internal force distribution change becomes more noticeable and different when the bracing affect is more resulting serious damage of adjacent columns than other columns (Sun, Zhang & Cao, 2013).

A two reinforced concrete frame models consist of five layers, one model involving two types of staircase and the other one does not involve staircase. The models are established to conduct the common earthquake effect of elastic time history analysis, of the frame force resulted from collaborate of board type stairs and frame is discussed. The analysis results indicate that the frame force changes mainly in the parts directly linking to board type stairs, the force in the beams, columns and boards

of the stairs rises clearly comparing with their static force (Zhang, Zhang & Tian, 2013).

Chapter 3

METHDOLOGY

3.1 Introduction

In the purpose of inspecting the impact of the staircase and its location on the reinforced concrete buildings performance Linear Static, Pushover nonlinear static and Time History analyses are suggested to be conducted. Four reinforced concrete buildings are modelled by ETABS-2016. These four models contain a staircase with four different locations, and in addition to that the same four buildings are modelled without considering a staircase.

3.2 Modelling by ETABS-2016

Initially eight models are designed by utilizing ETABS-16, model A, model B, model C and model D are modelled with considering staircase in four different locations, furthermore, model A-1, model B-1, model C-1 and model D-1 are modelled without considering staircase.

3.2.1 Geometrical Properties

The eight models have the common geometrical properties as following:

- Storey height 3.06 m.
- Number of storeys are eight.
- Number of bays in X direction are five.
- Number of bays in Y direction are three.
- Column section is $30 \times 80\ cm$

- Beam section is $30 \times 60\ cm$
- Slab thickness is $20\ cm$

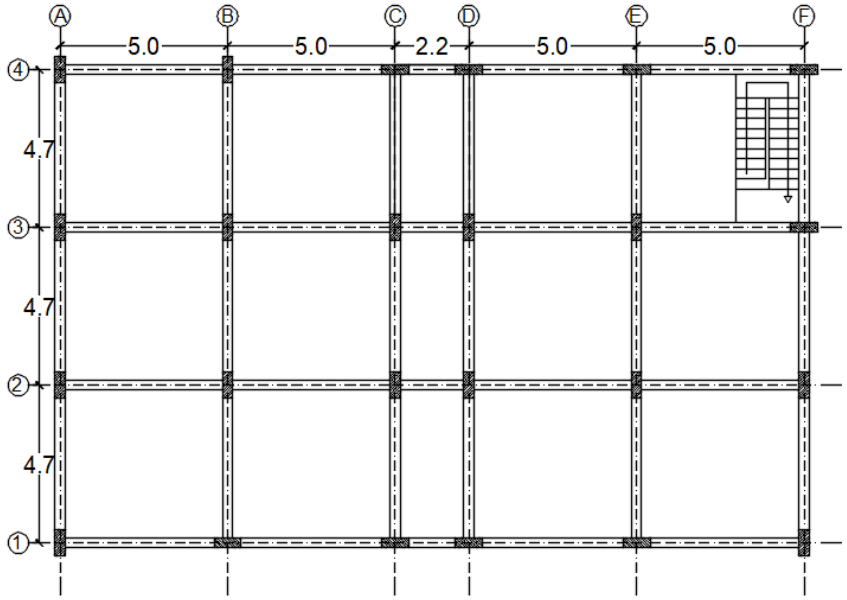

Figure 3.1: Plan view of building A.

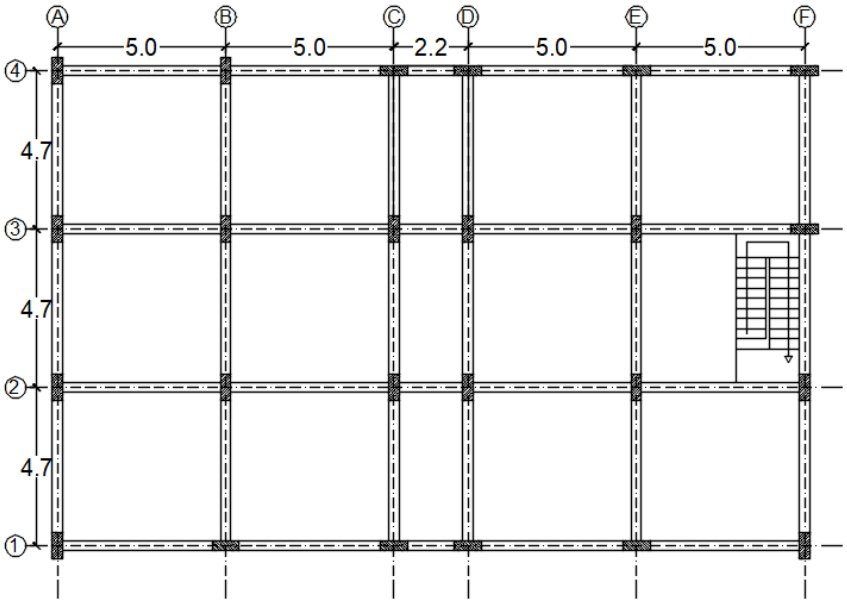

Figure 3.2: Plan view of building B.

As mentioned before, eight reinforced concrete buildings will be modelled and designed, four of these buildings with staircase and the other four buildings without staircase, in other words the place of staircase is empty. The Figures from 3.1-3.4

display the buildings A, B, C and D which contain staircase, furthermore, the columns, beams and slabs distribution are shown.

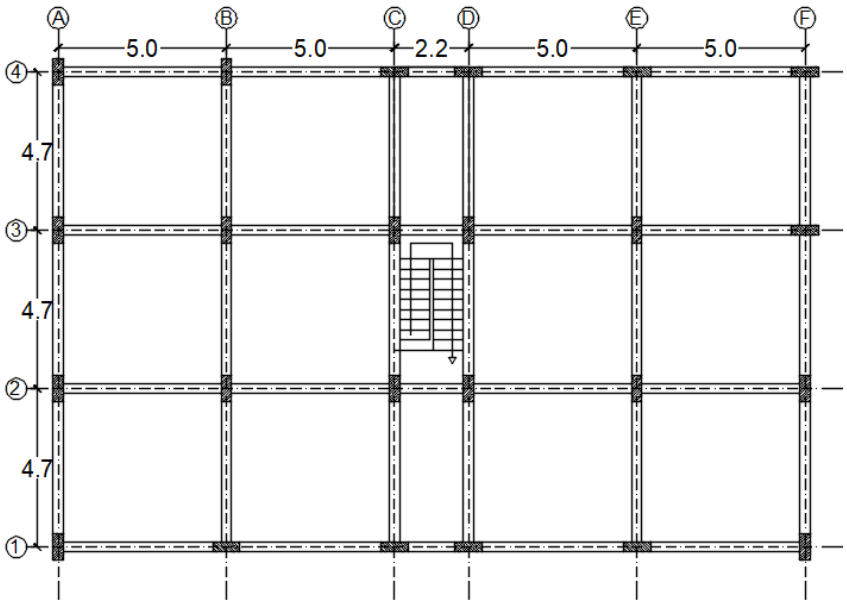

Figure 3.3: Plan view of building C.

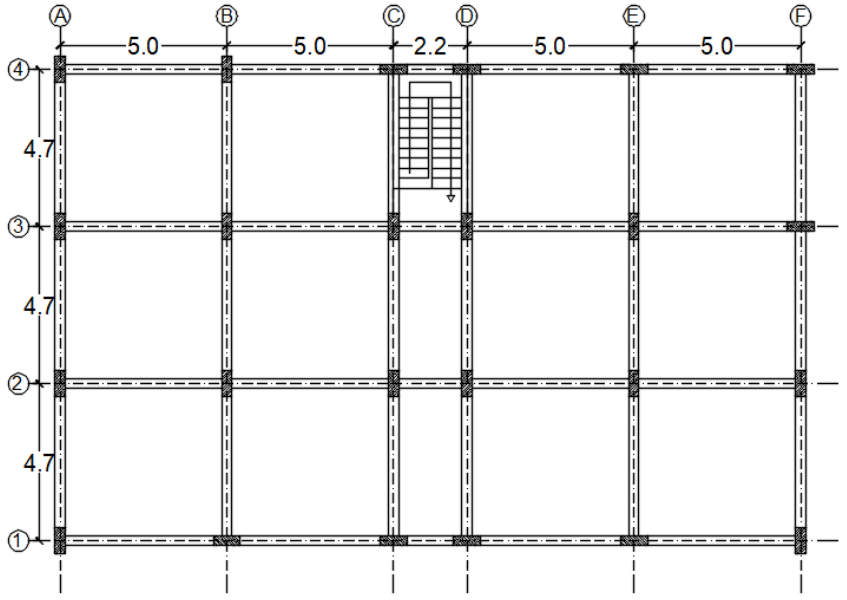

Figure 3.4: Plan view of building D.

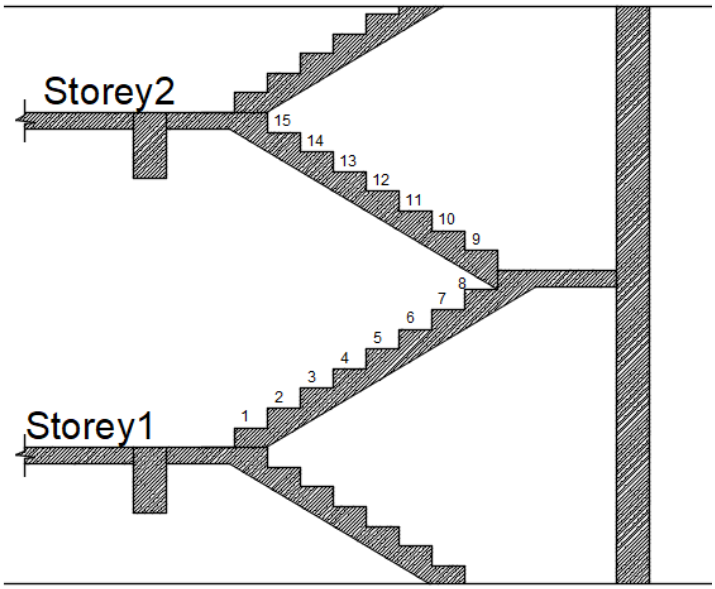

Figure 3.5: Section view of staircase.

3.2.2 Codes and Standards

- TS 500-2000 for the concrete design.
- TSC 2007 for the calculations of Earthquake loads.
- TS 498-97 for the load assumptions.
- Improvement of nonlinear static seismic analysis procedures FEMA440.
- Pre-standard and commentary for the seismic rehabilitation of buildings FEMA356.

3.2.3 Loading

The building function is a residential building, therefore, the live load is selected as $LL = 2\ kN/m^2$. The dead load is the self-weight of the structure which can be calculated by ETABS-2016, moreover, additional dead load is considered as $DL = 1.5\ kN/m^2$.

3.2.4 Material Properties

The concrete properties are as following:

- Compressive strength is 30 N/mm^2.
- Specific weight density is 25 kN/m^3.
- Modulus of elasticity is 31000 N/mm^2.

The steel (rebar) properties are as following:

- Specific weight density is 78 kN/m^3.
- Modulus of elasticity is 200000 N/mm^2.

3.3.5 Earthquake Parameters

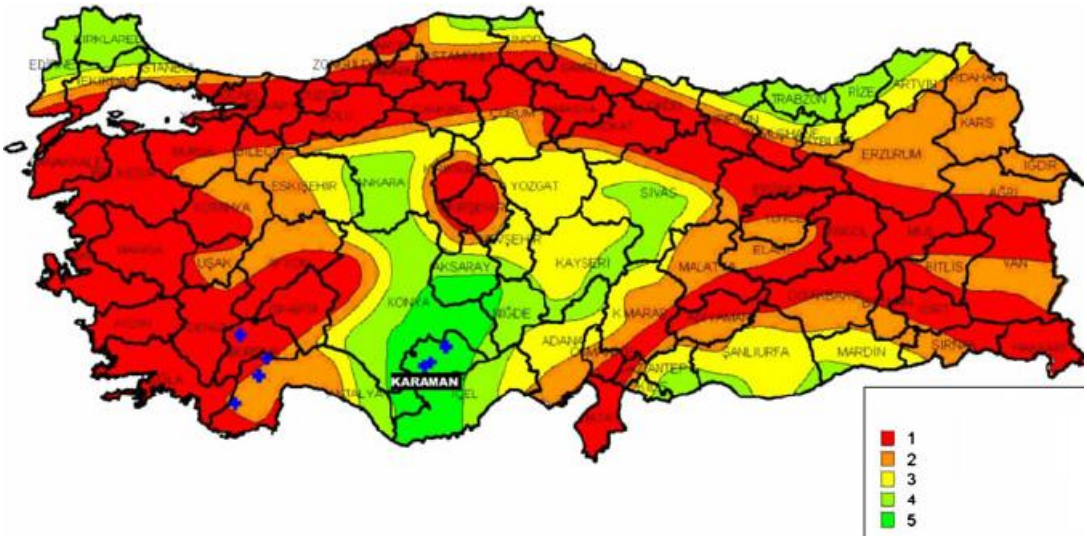

Figure 3.6: Earthquake map of Turkey.

Figure 3.5 demonstrates the earthquake regions map of Turkey, the region one which in red colour is the most dangerous zone. The building is placed in zone 1 for the purpose of investigating its performance in worst scenario.

The effective ground acceleration coefficient $A_0 = 0.4$ which related to the seismic zone 1 according to Turkish earthquake code 2007 as explained in Table 3.1.

Table 3.1: Effective ground acceleration coefficient (A_0) (TSC, 2007).

Seismic zone	$\boldsymbol{A_0}$
1	0.4
2	0.3
3	0.2
4	0.1

To select the local site class firstly soil group must be identified with respect to Table 3.2 that is classify the soil according to topmost layer thickness, thus the soil site class is chosen as Group (D) soils with h_1> 10 m.

Table 3.2: Local site class (TSC, 2007).

Local site class	**Soil group, according to topmost layer thickness ($\boldsymbol{h1}$)**
Z1	Group (A) soils Group (B) soils with $h_1 \leq$15m
Z2	Group (B) soils with $h_1 \geq$15m Group (C) soils with $h_1 \leq$15m
Z3	Group (C) soils with 15m < $h_1 \leq$ 50m Group (D) soils with $h_1 \leq$ 10m
Z4	Group (C) soils with $h_1 >$50m Group (D) soils with $h_1>$ 10m

The local site class is selected as $Z_4 = 0.4$ which defines the spectrum characteristic periods (T_A, T_B) according to Turkish earthquake code 2007 as explained in Table 3.3.

Table 3.3: Spectrum characteristic periods (T_A, T_B) (TSC, 2007).

Local site classification	$\mathbf{T_A}$, (**second**)	$\mathbf{T_B}$, (**second**)
Local site ,(Z 1)	0.10	0.30
Local site ,(Z 2)	0.15	0.40
Local site ,(Z 3)	0.15	0.60
Local site ,(Z 4)	0.20	0.90

The importance factor (I) of the building is depended on the function or type of the structure. In this study the importance factor of the building is selected as $I = 1$ with respect to Table 3.5 below.

Table 3.4: Building importance factor (TSC, 2007).

Function or Type of Building	**(Importance Factor)**
1. Buildings required to be used after the earthquake and buildings involving hazardous material: a) Buildings required to be used directly after the earthquake (Hospitals and dispensaries). b) Buildings involving or storing Toxic, explosive and flammable materials.	1.5
2. Intensively and long-term occupied buildings: a) Schools, other educational buildings and facilities, dormitories and hotels, military barracks, prisons. b) Museums.	1.4
3. Intensively but short-term occupied buildings: Cinema, Sport facilities, and concert halls.	1.2
4. Other buildings.	1

Structural system behavior factor R is related to the building structural system since the structural system of the building is moment frames type in this study, therefore, the structural system behavior factor is specified as $R = 8$. According to previous tables the earthquake parameters are summarized in Table 3.5.

Table 3.5: Earthquake parameters.

Earthquake parameters	**Value**
Seismic zone	1
Effective ground acceleration coefficient (A_0)	0.4
Building importance factor (I)	1
Soil class (Z)	Z4
Spectrum characteristic periods	$T_A = 0.2$, $T_B = 0.9$
Structural system behavior factor R	8

There are three formulas to specify the spectrum coefficient, which is depended on natural period of the building and the local site class condition. Figure 3.7 shows the spectrum coefficient $S(T)$. Spectrum coefficient should be calculated according to the following formulas

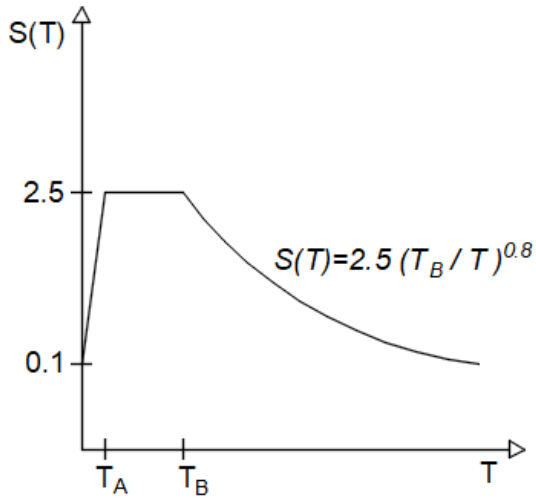

Figure 3.7: Spectrum coefficient curve (TSC, 2007).

$$S(T) = 1 + 1.5\frac{T}{T_A} \qquad if\ (0 \le T \le T_A) \tag{3.1}$$

$$S(T) = 2.5 \qquad if\ (T_A \le T \le T_B) \tag{3.2}$$

$$S(T) = 2.5\left(\frac{T_B}{T}\right)^{0.8} \qquad if\ (T_B \le T) \tag{3.3}$$

3.4 Analysis Methods

3.4.1 Linear Static Procedure (LSP)

When a body is subjected to loads, the body deforms and the impact of loads is transferred throughout it. Internal forces and reactions are encouraged by external loads in order to deliver the body into a situation of equilibrium. Displacements, strains, stresses, and reaction forces are computed by Linear Static Analysis under the impact of applied loads. A linear static analysis is defined as an analysis where a linear relation holds between applied forces and displacements as shown in Figure 3.8.

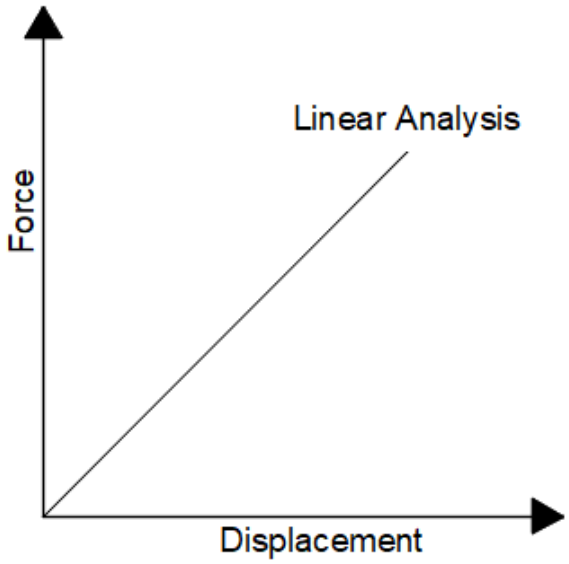

Figure 3.8: Force vs. displacement in Linear Static Analysis.

The stiffness matrix of the model in a linear static analysis is constant, and the solving process is comparatively short compared to a nonlinear analysis on the same model. Therefore, for a first estimate, the linear static analysis is firstly conducted then a full nonlinear analysis can be performed.

3.4.1.1 Equivalent Seismic Load Method

Equivalent seismic load method can be conducted to buildings that exists in seismic zone 1 in case of the torsional irregularity ratio coefficient satisfies the condition $\eta_{bi} \leq 2$ in all storeys and the total high limit satisfies the condition $H_N \leq 25$. The base shear (V_t) which is the equivalent seismic load acting on the building in the earthquake directions can be calculated by the following equation:

$$V_t = \frac{WA(T_1)}{R_a(T_1)} \geq 0.10\, A_0\, I\, W \tag{3.4}$$

The total weight of the building can be determined by the following Equation

$$W = \sum_{i=1}^{N} w_i \tag{3.5}$$

Where, w_i is storey weight of i^{th} storey and storey weight w_i shall be calculated according to Equation 3.6.

$$w_i = g_i + n\, q_i \tag{3.6}$$

Live load participation factor n is 0.3 according to TSC-2007 since the building function is residential as shown in Table 3.6.

Table 3.6: Live load participation factor (TSC, 2007).

Purpose of occupancy of building	$\boldsymbol{n}$
Depot, warehouse, etc.	0.6
School, dormitory, sport facility, cinema, theatre, concert hall, car park, restaurant, shop, etc.	0.8
Residence, office, hotel, hospital, etc.	0.3

Total equivalent seismic load is calculated by Equation 3.7.

$$V_t = \Delta F_N + \sum_{i=1}^{N} F_i \tag{3.7}$$

The equivalent seismic load ΔF_N which is the load acting in the top storey of the building is computed by

$$\Delta F_N = 0.0075\, N\, V_t \tag{3.8}$$

The seismic loads are distributed to storeys according to Equation 3.9.

$$F_i = (V_t - \Delta F_N) \frac{w_i\, H_i}{\sum_{j=1}^{N} w_i\, H_i} \tag{3.9}$$

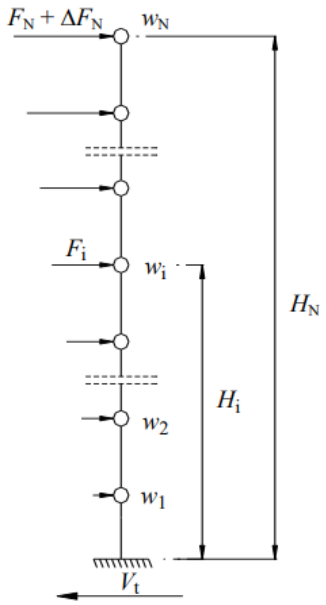

Figure 3.9: The distribution of the equivalent seismic loads to storeys (TSC, 2007).

The Figure 3.9 explains the allocation of equivalent seismic load of each storey with respect to Equation (3.9).

3.4.1.2 Irregular Buildings

Torsional irregularity A1 and inter-story stiffness irregularity B2 must be avoided in all models due to their negative seismic behavior.

Torsional Irregularity A1

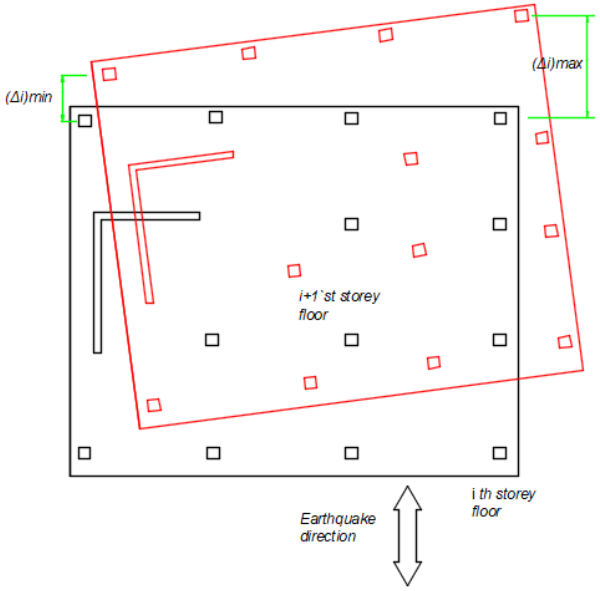

Figure 3.10: Torsional irregularity A1 (TSC, 2007).

The Figure 3.10 illustrates the A1 torsional irregularity. As shown, when equivalent seismic load is being applied the building starts to twist. Irregularity A1 occurs when the torsional irregularity Factor η_{bi} that is defined for any of the two orthogonal earthquake directions as the ratio of the maximum relative storey drift at any storey to the average relative storey drift at the same storey in the same direction, is larger than 1.2.

$$\eta_{bi} = (\Delta_i)max/(\Delta_i)avr \ > 1.2 \tag{3.10}$$

Where,

$$(\Delta_i)avr = 1/2[(\Delta_i)max/(\Delta_i)min\,] \tag{3.11}$$

When torsional irregularity A1 occurs at any storey level such that the torsional irregularity factor η_{bi} satisfies the Equation (3.12), then the ± 0.05 eccentricity ratio shall be amplified by multiplying it with coefficient D_i according to Equation (3.13).

$$1.2 < \eta_{bi} < 2 \tag{3.12}$$

$$D_i = \left[\frac{\eta_i}{1.2}\right]^2 \tag{3.13}$$

Inter-storey Stiffness Irregularity (Soft Storey) B2

B2 irregularity occurs when its factor η_{ki} that is described as the ratio of the average relative storey drift at any i^{th} storey to the average relative storey drift at the storey immediately above or below, is larger than 2 as shown in the following equations:

$$\eta_{ki} = \left(\frac{\Delta_i}{h_i}\right) avr / \left(\frac{\Delta_{i+1}}{h_{i+1}}\right) avr \ > 2 \tag{3.14}$$

$$\eta_{ki} = \left(\frac{\Delta_i}{h_i}\right) avr / \left(\frac{\Delta_{i-1}}{h_{i-1}}\right) avr \ > 2 \tag{3.15}$$

3.4.2 Non-Linear Static Procedure (NSP)

The nonlinear static analysis is commonly authoritative method to describe the structure behavior than the linear procedures. Nevertheless, the nonlinear static method cannot be precisely accounted for higher mode effects and for changes in dynamic response as the structure degrades in stiffness. When the seismic analysis of the building is decided to be nonlinear static analysis method, a mathematical model immediately integrating the nonlinear load-deformation characteristics of individual components. The target displacement shall be exceeded by applying monotonically increasing lateral loads representing inertia forces in an earthquake to the building elements.

In nonlinear static procedure (NSP) the three dimensional model accounts immediately for effects of material inelastic behaviour, the measured internal forces is not approximately realistic for those predictable through the design earthquake.

Therefore, the target displacement is aimed to characterise the maximum displacement to be experienced during the design earthquake.

3.4.2.1 Pushover Capacity Curve

The building ability under lateral forces is illustrated by pushover capacity curve. The capacity curve is shown in Figure 3.10, The Y axis represents the lateral load on the structure and X axis signifies the lateral deflection of the building roof. The hinge status and performance point of the structure can be obtained from the pushover capacity curve.

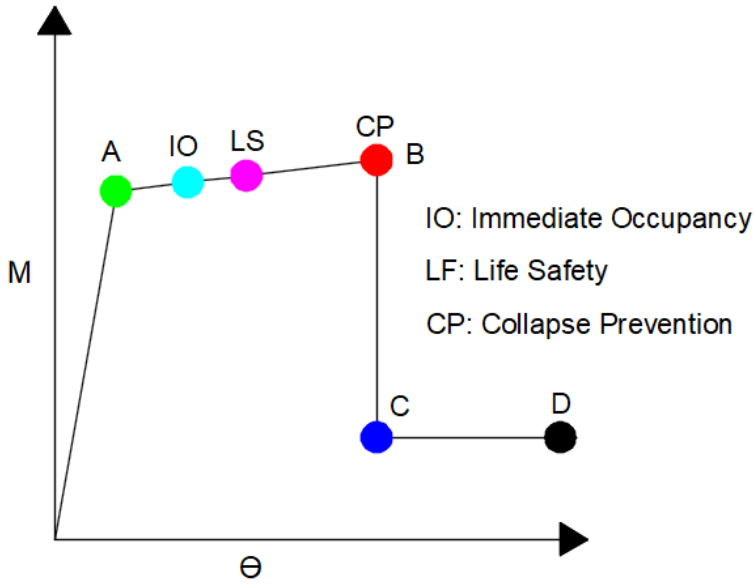

Figure 3.11: Plastic hinge phases.

The Figure 3.10 displays the performance level of any plastic hinge. The line between point A and IO represents the immediate occupancy level, the line between IO and LS signify the life safety level, the collapse prevention level is illustrated by the line between LS and CP, the line between point B and point C present the damage level, the line between point C and point D present the emergency level.

Immediate occupancy level

Immediate occupancy level is determined in case of the structural damage is very inconsiderable. The possibility of the risk of life injury and structure destruction is very low when the performance level of the structure is immediate occupancy level, in addition to that repairing of some structure element may be probable.

Life safety

Life safety level is determined in case of the structural damage is very considerable, however some structural elements or part of these elements still have the ability to resist collapse. The possibility of the risk of life injury could be exists, but generally the total risk of life injury due to the structure destruction is low. Repairing in life safety level is possible, however it is not recommended for economic reasons.

Collapse prevention

Collapse prevention level is reached when the structure is on the edge of facing partial or total collapse. Considerable degradation in the stiffness, extensive damage to the building is occurred and degradation in strength of the lateral force resisting system. In addition to that degradation in vertical load carrying capacity and great permanent lateral deformation of the structure. For the risk of life injury possibility is serious since the falling hazards from structure debris could occur.

Performance point

The performance point of the structure is defined as the intersection point of capacity curve with demand curve as illustrated in Figure 3.12, when the performance point of the building is occurred the performance level can be specified.

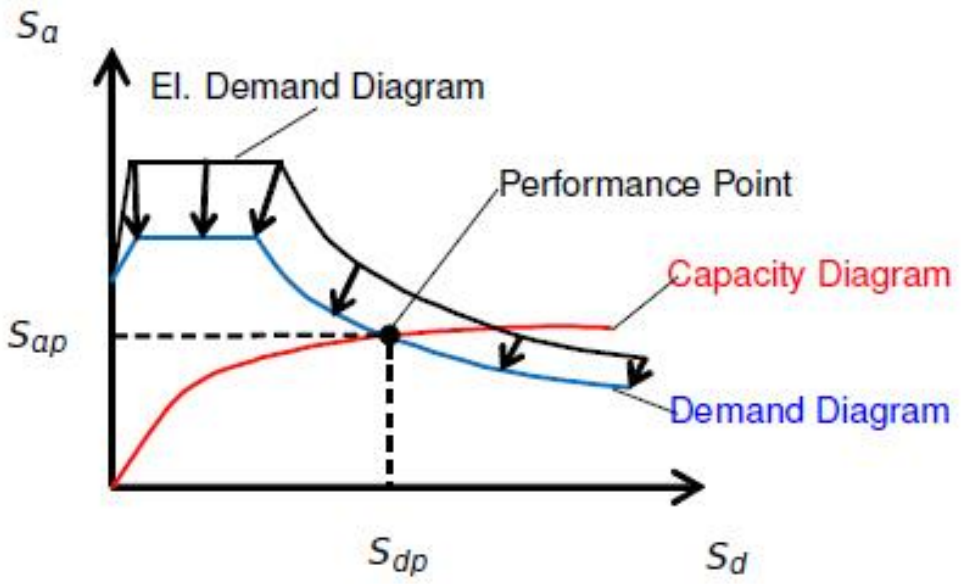

Figure 3.12: Performance point curve.

The Capacity Diagram embodies the structure nonlinear behaviour. It is also a load-deformation curve of the base shear force versus the structure horizontal roof displacement. The Demand Diagram represents a probable future earthquake with specific returning period, it is obtained by defining spectrum.

Effective lateral stiffness and effective yield strength

In order to attain the effective yield strength and the effective lateral stiffness of the structure the nonlinear force-displacement relationship between the base shear and displacement of the control node should be changed to bilinear relationship as shown in Figures 3.13 and 3.14. K_e indicates to effective lateral stiffness of the structure whereas K_i indicates to elastic lateral stiffness of the building, V_y represents the effective yield strength.

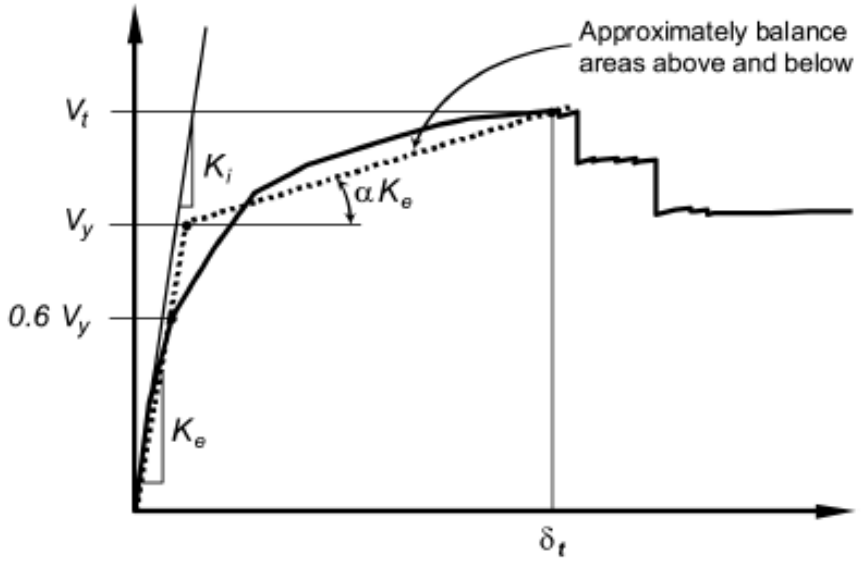

Figure 3.13: Idealized Force-Displacement Curve positive post-yield slope (FEMA356).

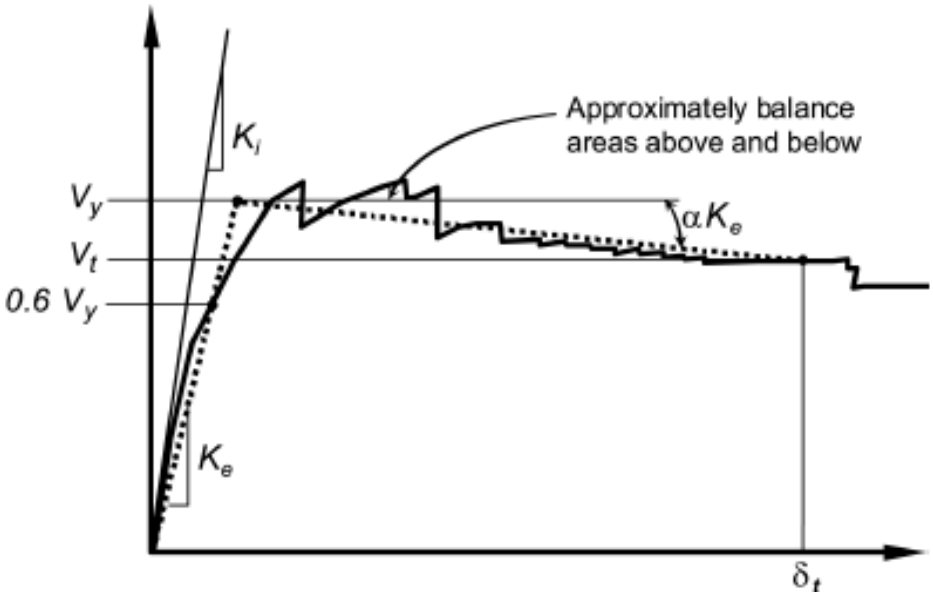

Figure 3.14: Idealized Force-Displacement Curve negative post-yield slope (FEMA356).

3.4.2.3 Analysis Considerations

The idealized force-displacement curve which represent the relation between base shear force and lateral displacement of the control node should be set up for control node displacements ranging between zero and 150% of the target displacement δ_t.

Loading

The mathematical model shall involve the component gravity loads, lateral-loads should be subjected in both orthogonal directions as shown in Figure 3.15, and for the design earthquake the maximum seismic effects should be utilized.

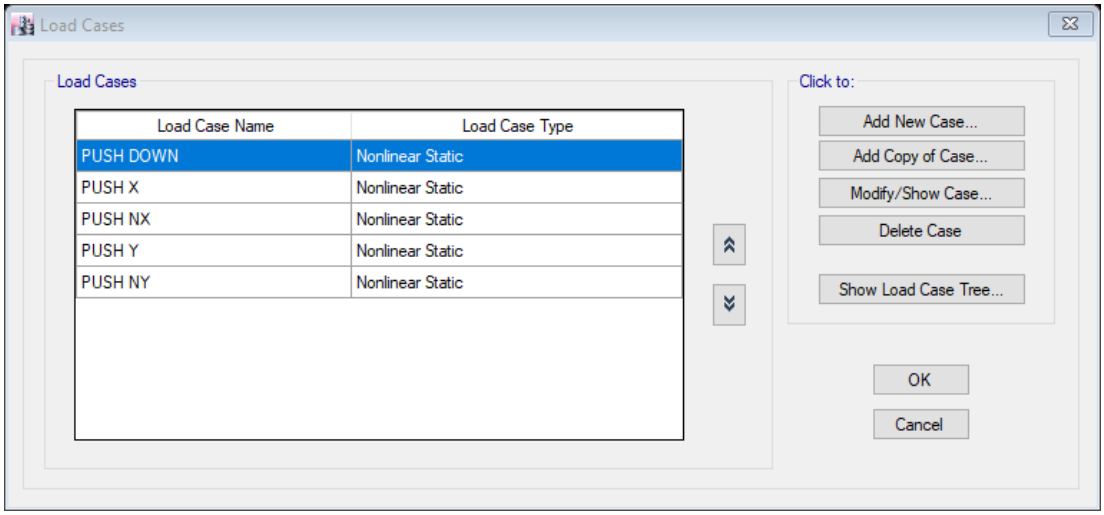

Figure 3.15: Defining lateral loads in both orthogonal directions in ETABS-2016.

For determining combination with seismic loads the following component gravity forces Q_G, should be deemed, the gravity loads should be attained with respect to Equation (3.16) when the gravity effects and seismic loads are additive.

$$Q_G = 1.1(Q_D + Q_L + Q_S) \tag{3.16}$$

The gravity loads should be observed according to Equation (3.17) in case of the gravity effects and seismic loads are counteracting

$$Q_G = 0.9Q_D \tag{3.17}$$

Where,

Q_D is the dead load.

Q_L is the effective live load equal to 25% of the unreduced design load.

Q_S is the effective snow load.

In this study only dead loads (self-weight of the building and additional dead load) and live load are considered as shown in Figure 3.16. Thus, the gravity loads shall be obtained according to the following equations

$$Q_G = 1.1(\,0.9\,Q_D + 0.25\,Q_L) \tag{3.18}$$

$$Q_G = \,Q_D + 0.3\,Q_L \tag{3.19}$$

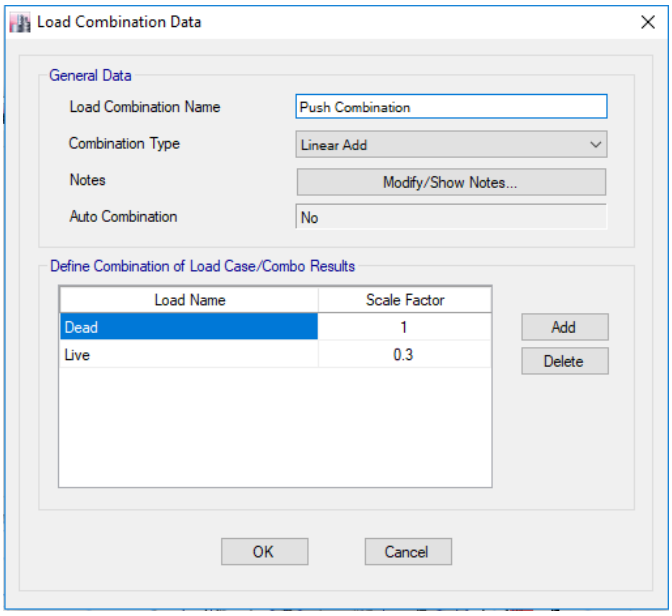

Figure 3.16: Defining the gravity loads combination in ETABS-2016.

Control node assignment

The control node displacement in the model should be obtained for the lateral loads. The control node should be defined at the mass centre of the building at top storey.

The following figure explains defining the displacement control node at centre of mass at top storey in one of the models in this study.

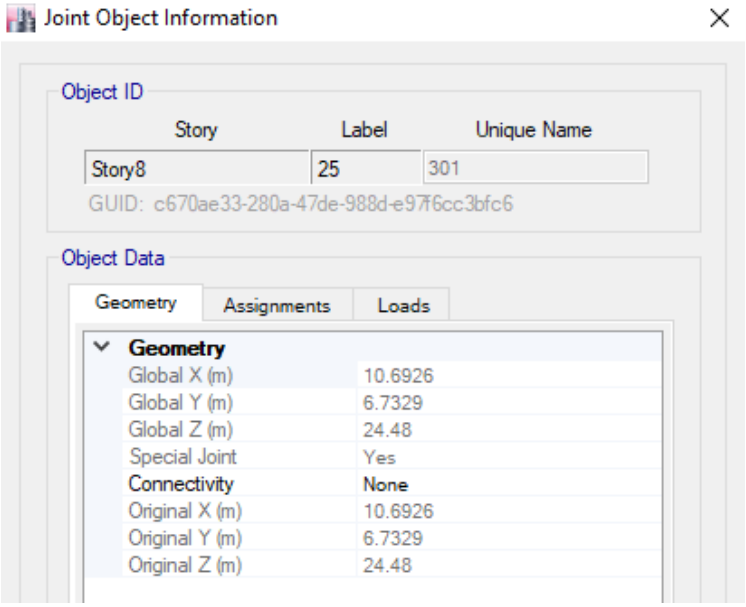

Figure 3.17: Defining the displacement control node in ETABS-2016.

Hinge assignment

Assign hinge properties existing in ETABS Nonlinear as per ATC-40 to the columns and beams. The column that yields based upon the interaction of axial force and bending moment (P-M2-M3) as shown in Figure 3.18.

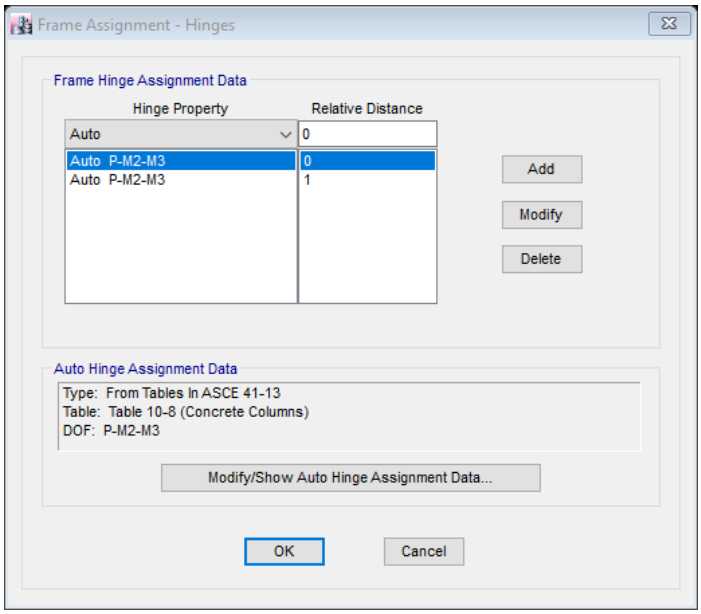

Figure 3.18: Column hinge assignment data.

The beam hinge that yields based upon the flexure (M3) is assigned as displayed in Figure 3.18.

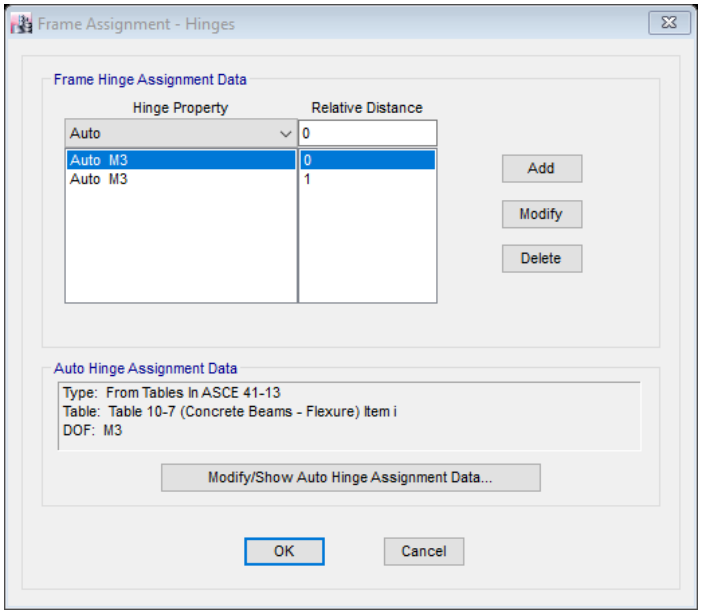

Figure 3.19: Beam hinge assignment data.

Target displacement calculation

The target displacement δ_t is proposed to characterise the maximum displacement to be experienced through design earthquake. In case which building diaphragms are

rigid in all floors level, the target displacement can be obtained according to Equation (3.20) (FEMA-356).

$$\delta_t = C_0 C_1 C_2 C_3 S_a \frac{T_e^2}{4\pi^2} \ g \tag{3.20}$$

$C_0 =$ Modification factor to relate spectral displacement to the roof displacement of the building. The modification factor is selected to be 1.46 in accordance to Table 3.7, linear interpolation method is applied to calculate C_0 since the building is consisted of eight storeys.

Table 3.7: C_0 Modification factor values (FEMA-356).

	Shear Building		**Other Building**
(Number of Stories)	**(Triangular Load Pattern)**	**(Uniform Load Pattern)**	**(Any Load Pattern)**
1	1	1	1
2	1.2	1.15	1.2
3	1.2	1.2	1.3
5	1.3	1.2	1.4
10+	1.3	1.2	1.5

C_1 defined as modification factor to relate expected maximum inelastic displacements to displacements obtained for linear elastic response, C_1 is calculated with respect to Equation (1.21) or (1.22).

$$C_1 = \ 1 \text{ for } T_e \geq T_S \tag{3.21}$$

$$C_1 = \ [1 + (R-1)T_S/T_e]/\text{R for } T_e < T_S \tag{3.22}$$

Where,

T_S is defined as characteristic period of the response spectrum.

T_e is the effective fundamental period of the building in the direction under consideration. R is defined as ratio of elastic strength demand.

For specifying C_2 factor which represents the impact of pinched hysteretic shape, stiffness degradation and strength deterioration on maximum displacement response.

Table 3.8: C_2 Modification factor values (FEMA-356).

Structural Performance Level	$T \leq 0.1\ second$		$T \geq T_S\ second$	
	Framing Type1	Framing Type2	Framing Type1	Framing Type2
Immediate Occupancy	1	1	1	1
Life Safety	1.3	1	1.1	1
Collapse Prevention	1.5	1	1.2	1

Where framing type 1 is representing the structures in case of more than 30% of the storey shear is resisted by any of the combination of the following components, elements, or frames: ordinary moment-resisting frames, concentrically-braced frames, frames with partially-restrained connections, tension-only braces, unreinforced masonry walls, shear-critical, piers, and spandrels of reinforced concrete or masonry. Thus, in this study the C_2 factor is selected to be 1.1 since the structure performance target is life safety. Framing type 2 is embodies the frames that are not mentioned in framing type 1.

For determining C_3 modification factor which display the increased displacements as a result of dynamic P-Δ effects. C_3 factor should be chosen as 1 for building with positive post-yield stiffness, therefore C_3 value is set up to be 1 in this study.

For obtaining S_a that represents the response spectrum acceleration, at the effective fundamental period and the building damping ratio in the direction under consideration. In this study S_a factor shall be calculated in accordance with the following equations according to Turkish earthquake code 2007.

$$S_a(T) = A(T)\, g \tag{3.23}$$

$$A(T) = A_0\, I\, S(T) \tag{3.24}$$

The last factor g in target displacement equation is the acceleration of gravity. After observing all modification factors, the target displacement can be calculated according to equation as displayed in Table 3.9

Table 3.9: Calculations of modification factors and the target displacement for each model.

Model name	**Direction**	C_0	C_1	C_2	C_3	A_0	S_a	T_e	δ_t (m)	δ_t (mm)
Model A	X	1.46	1.2	1.1	1	0.4	1	0.757	0.276	276
	Y	1.46	1.4	1.1	1	0.4	1	0.664	0.242	242
Model A-1	X	1.46	1.2	1.1	1	0.4	1	0.767	0.280	280
	Y	1.46	1.3	1.1	1	0.4	1	0.702	0.256	256
Model B	X	1.46	1.2	1.1	1	0.4	1	0.758	0.276	276
	Y	1.46	1.4	1.1	1	0.4	1	0.665	0.242	242
Model B-1	X	1.46	1.2	1.1	1	0.4	1	0.766	0.279	279
	Y	1.46	1.3	1.1	1	0.4	1	0.705	0.257	257
Model C	X	1.46	1.2	1.1	1	0.4	1	0.733	0.267	267
	Y	1.46	1.4	1.1	1	0.4	1	0.649	0.237	237
Model C-1	X	1.46	1.2	1.1	1	0.4	1	0.762	0.278	278
	Y	1.46	1.3	1.1	1	0.4	1	0.709	0.258	258
Model D	X	1.46	1.2	1.1	1	0.4	1	0.741	0.270	270
	Y	1.46	1.4	1.1	1	0.4	1	0.653	0.238	238
Model D-1	X	1.46	1.2	1.1	1	0.4	1	0.764	0.278	278
	Y	1.46	1.3	1.1	1	0.4	1	0.707	0.258	258

3.5 Time History Analysis

Ground motions are chosen and scaled to allow an analysis of the response history that supports design or performance evaluation. The usage of non-linear response-history analysis is conducted for designing new buildings and designing seismic upgrades of existing structures (Haselton, Whittaker, Hortacsu, Baker, Bray & Grant, 2012).

3.5.1 Scaling of Acceleration Spectrum

Reduced acceleration spectrum ordinate shall be calculated by Equation 3.25.

$$S_{aR} = \frac{S_{ae}(T_n)}{R_a(T_n)} \tag{3.25}$$

Where

$$S_{ae}(T_n) = A(T) \times g \tag{3.26}$$

The spectral acceleration coefficient $A(T)$ shall be determined in accordance with Equation 3.27. g is spectral acceleration coefficient with gravity.

$$A(T) = A_0 \times I \times S(T) \tag{3.27}$$

Spectrum coefficient S(T) can be determined by Equations (3.1, 3.2 and 3.3), the building importance factor $I = 1$ and the effective ground acceleration coefficient $A_0 = 0.4$ in this study since the seismic zone is one in according to Turkish Earthquake Code 2007.

$R_a(T_n)$ seismic load reduction factor shall be calculated according to Equation 3.28 or 3.29. In this study the seismic load reduction factor $R_a(T) = R = 8$.

$$R_a(T) = 1.5 + (R - 1.5) \times \frac{T}{T_A} \qquad (0 \leq T \leq T_A) \tag{3.28}$$

$$R_a(T) = R \qquad (T_A < T) \tag{3.29}$$

After determining all factors required the scaled acceleration spectrum is calculated as explained in Table 3.10.

Table 3.10: Acceleration spectrum calculation.

Period	**S(T)**	**A(T)**	$\boldsymbol{S_{aR}}$
0	1	0.4	0.4905
0.05	1.375	0.55	0.67444
0.1	1.75	0.7	0.85838
0.15	2.125	0.85	1.04231
0.2	2.5	1	1.22625
0.5	2.5	1	1.22625
0.6	2.5	1	1.22625
0.7	2.5	1	1.22625
0.9	2.5	1	1.22625
1	2.29792	0.91917	1.12713
2	1.31981	0.52792	0.64736
4	0.75803	0.30321	0.37181
8	0.43537	0.17415	0.21355
10	0.3642	0.14568	0.17864
15	0.26331	0.10532	0.12915
20	0.20918	0.08367	0.1026
30	0.15123	0.06049	0.07418

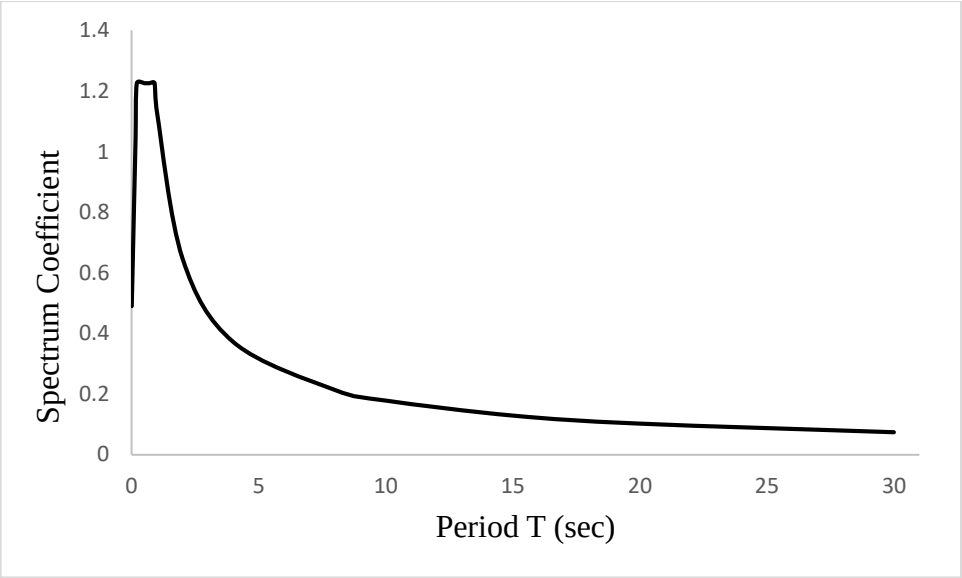

Figure 3.20: Scaled spectrum response shape.

Figure 3.20 shows the scaled spectrum response shape of structural models in this study. The local site class of all models is seismic zone one.

3.5.2 Selecting Real Earthquake Records

According to Turkish earthquake code at least three different ground motions should be selected to perform the time history analysis and the maximum results are discussed. In this study the Pacific earthquake engineering research (PEER) Center, NGA strong motion data base (PEER, 2005, http://peer.berkeley.edu/smcat) is used for selecting earthquakes records. The selected earthquakes are Duzce earthquake, Kocaeli earthquake and Izmir earthquake. All selected earthquake have the same local site classification which is seismic zone one.

Kocaeli earthquake

Kocaeli earthquake was in Kocaeli city in Turkey in 1999. The max magnitude earthquake magnitude was 7.51. The scaled response spectra of the earthquake is displayed in Figure 3.21.

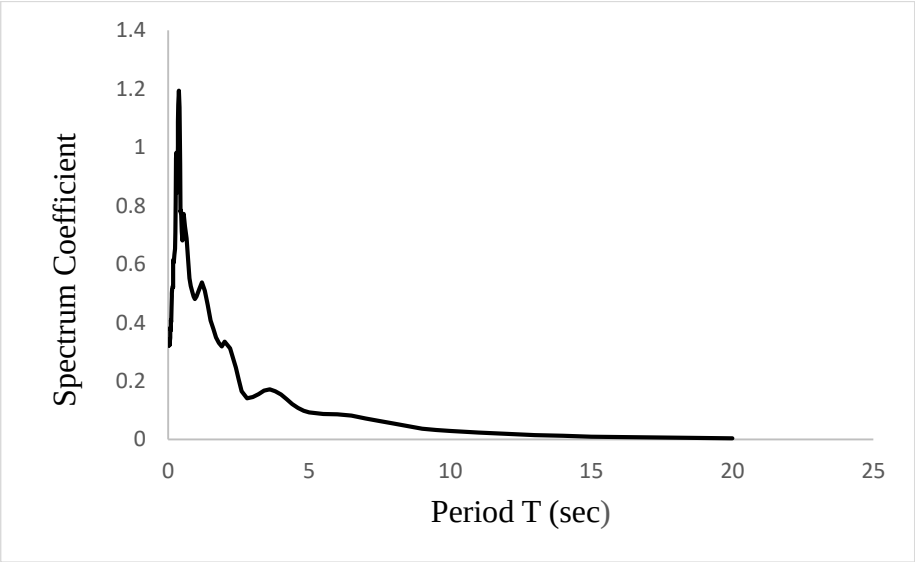

Figure 3.21: Scaled response spectra of Kocaeli earthquake 1999.

Duzce earthquake

Duzce earthquake was in Duzce city in Turkey in 1999. The max magnitude earthquake magnitude was 7.14. The scaled response spectra of the earthquake is demonstrated in Figure 3.22.

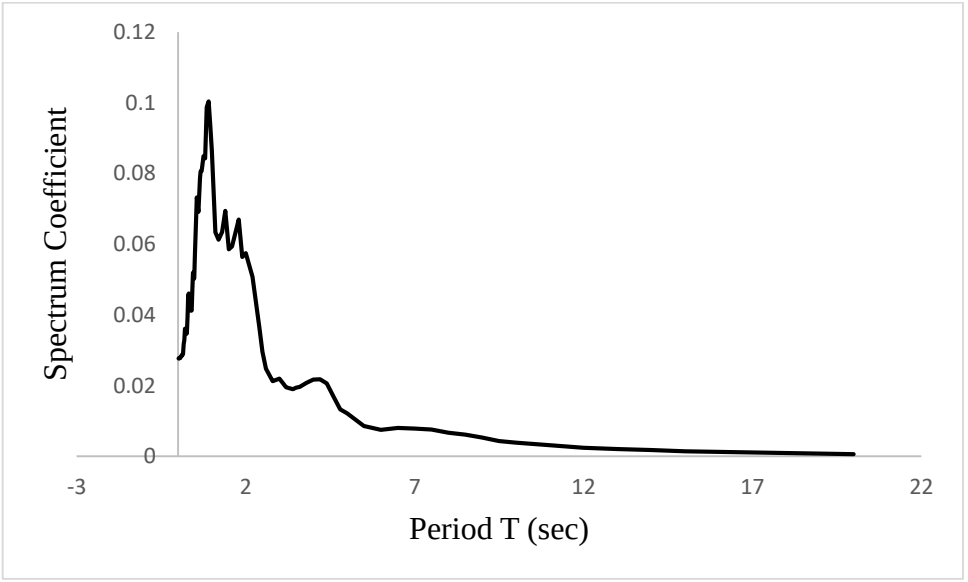

Figure 3.22: Scaled response spectra of Duzce earthquake 1999.

Izmir earthquake

Izmir earthquake was in Izmir city in Turkey in 1977. The max magnitude earthquake magnitude was 5.3. The scaled response spectra of the earthquake is demonstrated in Figure 3.23.

All earthquakes are defined in ETABS program and matched in frequency domain to the target response spectrum which is the spectral response of structural models in this study. The results of the Non-linear Time History analysis are compared in terms of diaphragm centre mass of displacements, max drift storey and the formation of plastic hinges in order to specify the most critical case.

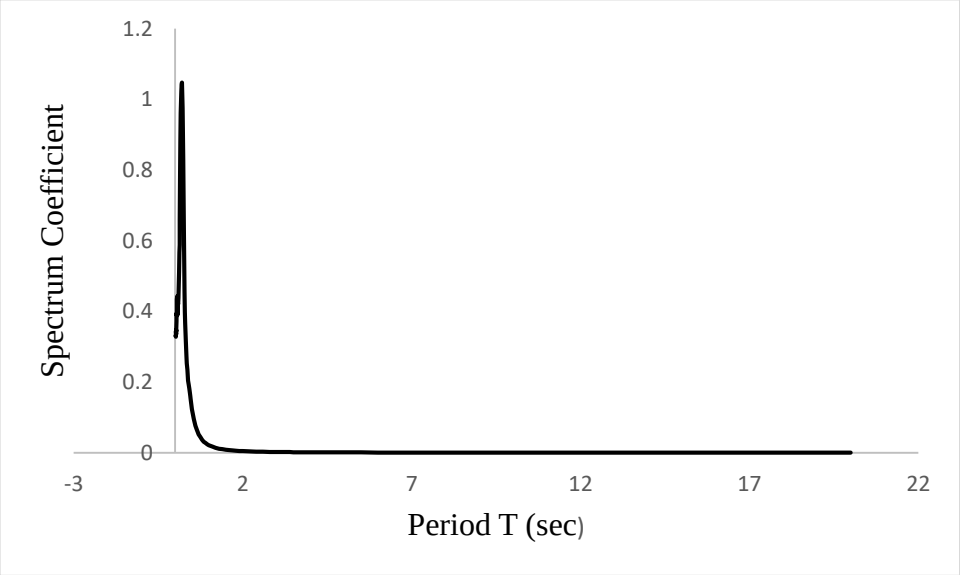

Figure 3.23: Scaled response spectra of Izmir earthquake 1977.

Chapter 4

REUSLTS AND DISSUCIONS

4.1 Introduction

Linear Static, Pushover nonlinear static and Time History analyses are conducted according to methodology which is explained in previous chapters to investigate the influence of the staircase presence and its location on the behaviour of eight storeys reinforced concrete building under lateral loads in both orthogonal directions. This chapter presents the outcomes and the discussions of both linear and nonlinear analyses, the obtained results from Linear Static analysis are compared in terms of torsional and inter-storey stiffness irregularities, reinforcement ratios. The obtained results from Pushover nonlinear static analyses are compared in terms of monitored displacements, spectral displacement, shear forces and stiffness. Finally Time History analyses results are discussed in terms of diaphragm center of mass displacements, storey drifts and formation of collapse prevention hinges.

4.2 Linear Static Analysis Results

This section includes the results and comparisons are made between models that contain staircase (model A, B, C and D) and models that do not involve staircase (model A.1, B.1, C.1 and D.1) in terms of torsional irregularity (A1), inter-storey stiffness (soft storey) irregularity (B2), and reinforcement ratios of columns that carry the staircase.

The Linear Static analysis is performed for four different lateral load cases. The first case is named as EPX, which refers that the earthquake load is in positive x-direction. The second case is named as ENX, which refers that the earthquake load is in negative x-direction. Similarly the third and fourth cases are in positive y- and negative y-directions.

4.2.1 Irregularities

4.2.1.1 Model A & A-1

Figure 4.1 displays the plan and 3D views of eighth storey building named model (A). The model (A) contains a staircase at the corner. Consequently, the weight and the stiffness of the stairs are also considered in the linear static analysis for the load combination which including the dead load, live load and the equivalent static earthquake load. The model (A.1) does not contain a staircase at the corner as shown in Figure 4.2. Therefore, the weight and the stiffness of the stairs are not considered in the linear static analysis.

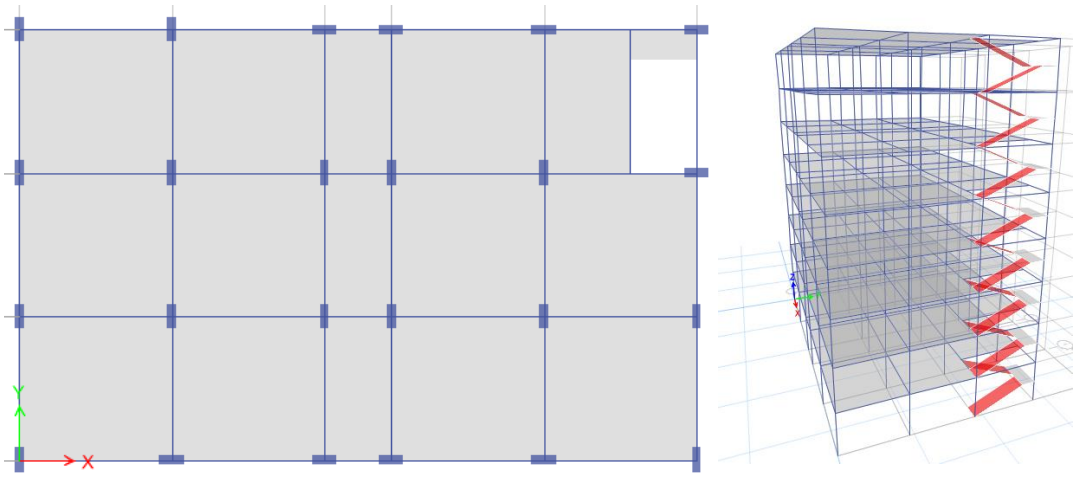

Figure 4.1: Plan view and 3D view of Model (A).

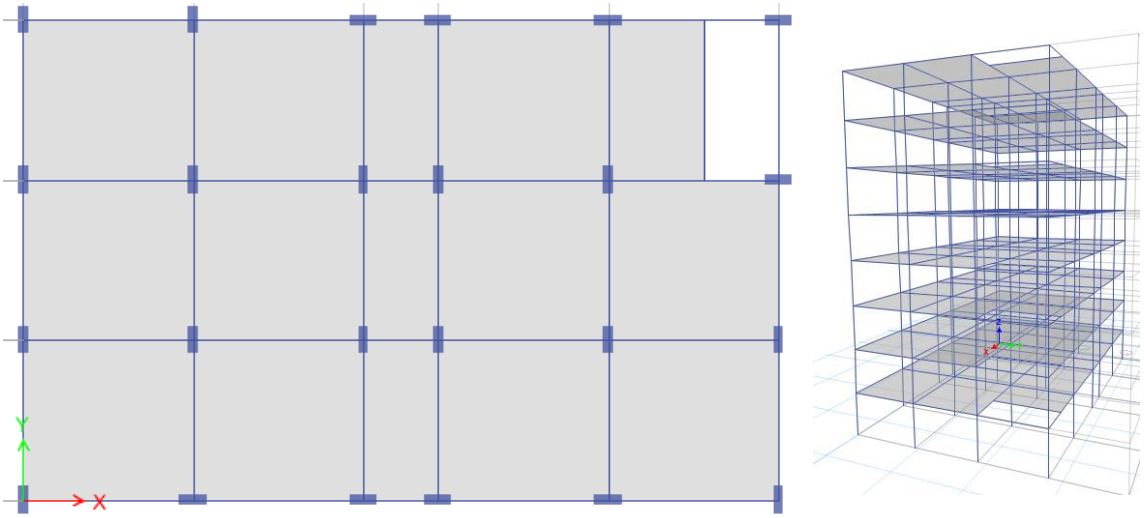

Figure 4.2: Plan view and 3D view of Model (A-1).

Irregularity (A1 & B2) checks

Table 4.1: A1 and B2 irregularity check for Model (A &A.1) in both orthogonal directions.

	Model (A)				**Model (A.1)**			
Load Case	η_{bi}	**A1**	η_{ki}	**B2**	η_{bi}	**A1**	η_{ki}	**B2**
EPX	1.067	√	1.53	√	1.071	√	1.53	√
ENX	1.028	√	1.52	√	1.049	√	1.53	√
EPY	1.036	√	1.53	√	1.245	*	1.59	√
ENY	1.2	√	1.53	√	1.085	√	1.60	√

√: Does not Exist, *: Exist

η_{bi}:Torsion Irregularity Factor

η_{ki}: Stiffness Irregularity Factor

As shown in Table 4.1, the torsional irregularity and inter-story stiffness irregularity are not existed in model A in both orthogonal directions, whereas in model A.1 torsional irregularity is existed in Y direction and inter-story stiffness irregularity is not existed in both orthogonal directions.

According to Turkish earthquake code 2007, when A1 irregularity exists at any storey, ± 5% eccentricity can be amplified if the drift ratio is more than 1.2 and less

than 2. Therefore, eccentricity in EPY direction shall be amplified since the drift ratio satisfies the Turkish earthquake code condition. By multiplying ± 5% eccentricity with a coefficient D_i which is presented in Equation 4.1, amplifying can be done.

$$D_i = \left[\frac{\eta_i}{1.2}\right]^2 \tag{4.1}$$

Table 4.2: Amplified eccentricity in EPY direction for Model (A-1)

Load Case	**Eccentricity**	$\boldsymbol{\eta_i}$	$\mathbf{D_i}$	**Amplified Eccentricity**
EPY	0.05	1.245	1.076406	0.054

The amplified eccentricity ratio is displayed in Table 4.2, the torsional factor is 1.245 more than 1.2 and less than 2 that is satisfies the condition of Turkish earthquake code 2007, therefore to obtain the magnified eccentricity the coefficient D_i shall be multiplied by the eccentricity ratio 0.05.

4.2.1.3 Model B & B-1

The staircase location in model B is illustrated in Figure 4.3, Figure 4.3 shows the plan and 3D views of model B, however, model B.1 that does not include staircase is displayed as plan and 3D views in Figure 4.4, the staircase place in model B-1 left empty.

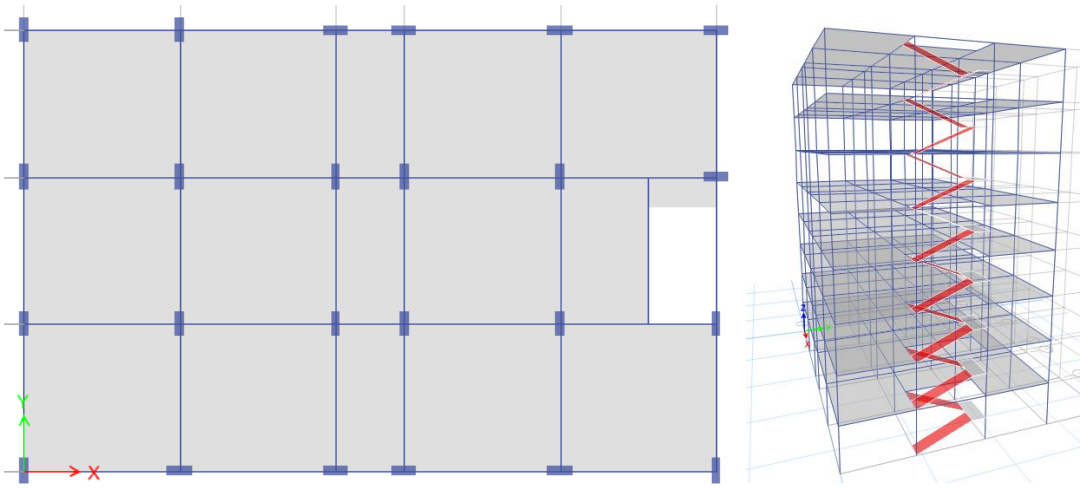

Figure 4.3: Plan and 3D view of model B.

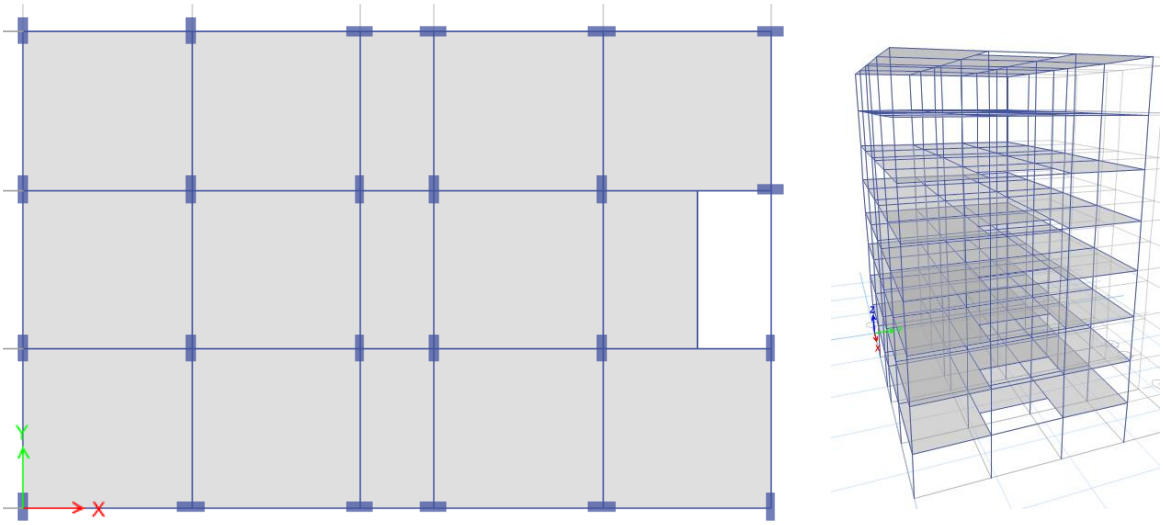

Figure 4.4: Plan and 3D view of model B-1.

Irregularity (A1& B2) Checks

Table 4.3: A1 and B2 irregularity check for Model (B &B-1) in both orthogonal directions.

	Model (B)				Model (B-1)			
Load Case	η_{bi}	**A1**	η_{ki}	**B2**	η_{bi}	**A1**	η_{ki}	**B2**
EPX	1.07	√	1.52	√	1.073	√	1.52	√
ENX	1.02	√	1.52	√	1.043	√	1.60	√
EPY	1.12	√	1.56	√	1.251	*	1.60	√
ENY	1.22	*	1.58	√	1.075	√	1.61	√

√: Does not Exist, *: Exist

η_{bi}: Torsion Irregularity Factor

η_{ki}: Stiffness Irregularity Factor

As explained in Table 4.3, in model B the torsional irregularity is occurred only in NY direction and inter-story stiffness irregularity is not occurred in both orthogonal directions. In model B-1 the torsional irregularity is existed in PY direction whilst the inter-story stiffness irregularity is not arisen in both orthogonal directions. The torsional irregularity factor in both models B and B-1 satisfies the Turkish earthquake codes 2007 condition of amplifying the eccentricity ratio.

Table 4.4: Amplified eccentricity in ENY and EPY directions of Model (B and B-1).

Model B					Model B-1			
Load Case	**(e)**	η_i	D_i	**A (e)**	**Load Case**	η_i	D_i	**A (e)**
ENY	0.05	1.22	1.04	0.052	**EPY**	1.25	1.09	0.054

e: Eccentricity

A: amplified

The amplified eccentricity is calculated for both models B and B.1 as shown in Table 4.4, the new eccentricity ratio of model B in negative Y lateral loads direction is 0.052, whereas in model B-1 the magnified eccentricity ratio is 0.054.

4.2.1.5 Model C & C-1

The plan view and three dimensional view of model C are illustrated in Figure 4.5, the staircase location is in the middle of the building. Figure 4.6 shows the plan view and three dimensional view of model C.1 that does not contain staircase.

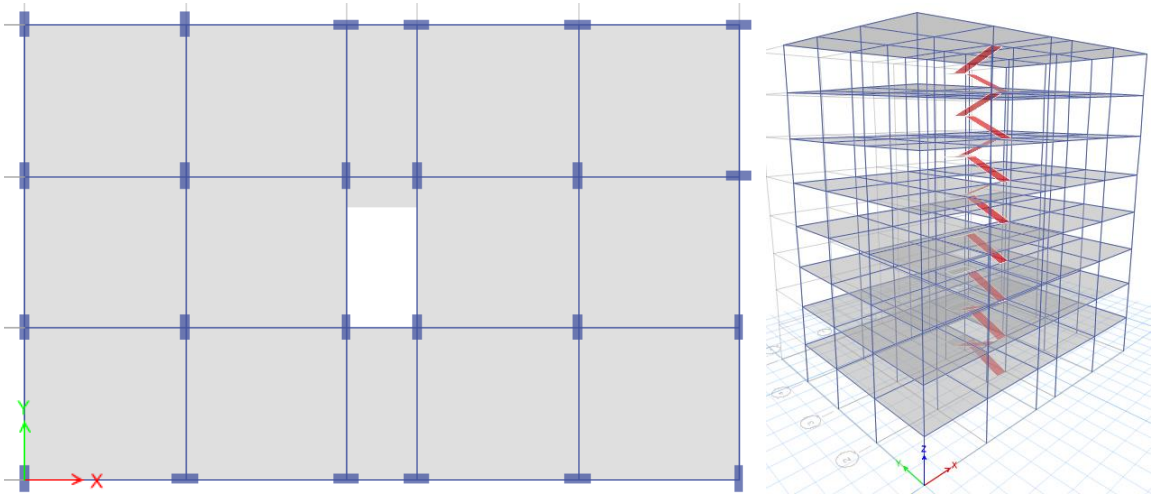

Figure 4.5: Plan view and 3D view of model C.

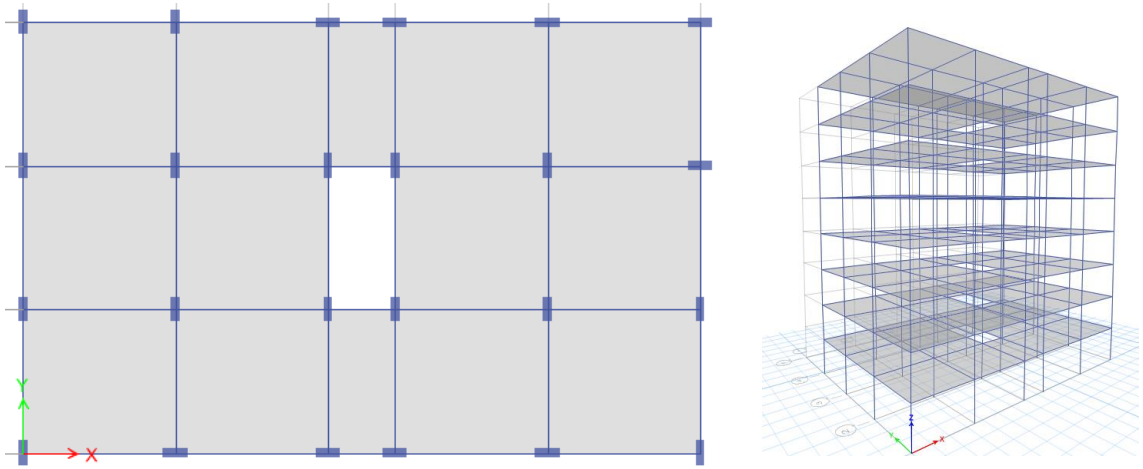

Figure 4.6: Plan view and 3D view of model C.1.

Torsional Irregularity (A1&B2) checks

The calculated torsional and inter-story stiffness factors for both models C and C.1 is shown in Table 4.5, in model C-1 the torsional factor in PY lateral load direction is more 1.2 that means the torsional irregularity is existed in PY direction while the inter-story stiffness factor in both orthogonal directions is less 2 that means the inter-story stiffness irregularity is not existed. For model C.1 the torsional factor in positive Y lateral load direction is greater than 1.2 therefore A1 irregularity is occurred, whereas inter-story stiffness factor is less than 2 which means B2 irregularity type is not existed. Since the torsional factors in both models C and C.1 is greater than 1.2 and less than 2 equation 1 is applicable in order to amplify the eccentricity ratio.

Table 4.5: A1 and B2 irregularity check for Model (C&C-1) in both orthogonal directions.

	Model (C)				**Model (C.1)**			
Load Case	η_{bi}	**A1**	η_{ki}	**B2**	η_{bi}	**A1**	η_{ki}	**B2**
EPX	1.071	√	1.50	√	1.072	√	1.52	√
ENX	1.047	√	1.50	√	1.043	√	1.52	√
EPY	1.324	*	1.54	√	1.289	*	1.60	√
ENY	1.089	√	1.55	√	1.06	√	1.61	√

√: Does not Exist, *: Exist

η_{bi}:Torsion Irregularity Factor

η_{ki}: Stiffness Irregularity Factor

Table 4.6: Amplified eccentricity in ENY and EPY directions of Models (C and C-1).

Model C					Model C.1			
Load Case	**(e)**	**η_i**	**D_i**	**A (e)**	**Load Case**	**η_i**	**D_i**	**A (e)**
ENY	0.05	1.324	1.22	0.061	**EPY**	1.289	1.15	0.058

e: Eccentricity

A: amplified

As clarified in Table 4.6, the amplified eccentricity ratios are calculated for both models C and C-1 in accordance to equation 1, the new eccentricity ratio of model C is 0.061 in negative Y lateral load direction, however the new eccentricity ratio of model C-1 is 0.058 in positive lateral load direction.

4.2.1.7 Model D & D-1

Figure 4.7 displays the plan and three dimensional view of the model D that involve staircase as show below. Figure 4.8 presents the model D-1 in plan and three dimensional views, the model D-1 does not contain staircase, the staircase place left empty.

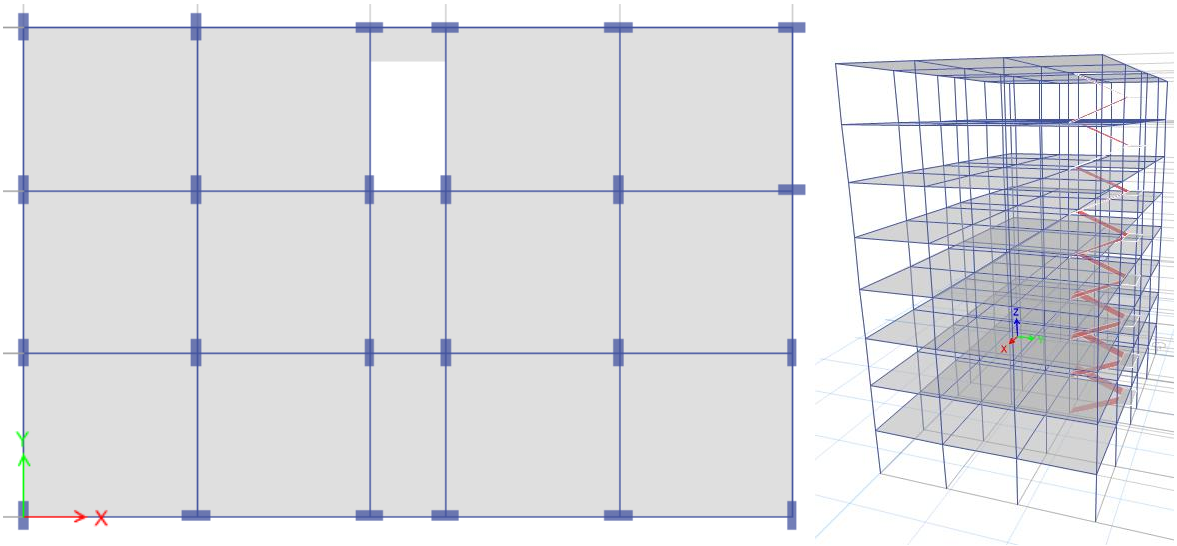

Figure 4.7: Plan view and 3D view of model D.

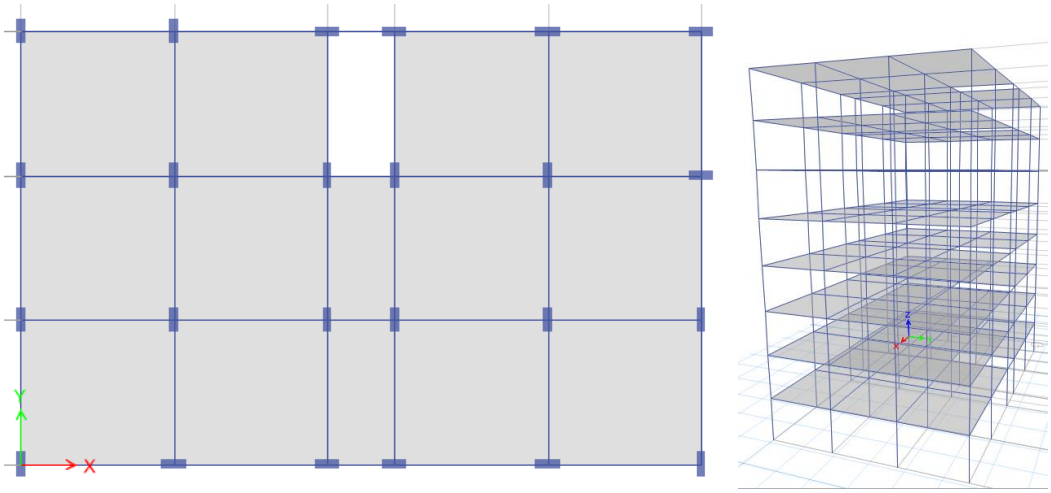

Figure 4.8: Plan view and 3D view of model D-1.

Torsional Irregularity (A1&B2) Checks

Table 4.7: A1 and B2 irregularity check for Model (D&D-1) in both orthogonal directions.

	Model (D)				Model (D-1)			
Load Case	**η_{bi}**	**A1**	**η_{ki}**	**B2**	**η_{bi}**	**A1**	**η_{ki}**	**B2**
EPX	1.072	√	1.51	√	1.06	√	1.51	√
ENX	1.043	√	1.51	√	1.04	√	1.52	√
EPY	1.29	*	1.54	√	1.26	*	1.60	√
ENY	1.06	√	1.55	√	1.06	√	1.61	√

√: Does not Exist, *: Exist

η_{bi}:Torsion Irregularity Factor

η_{ki}: Stiffness Irregularity Factor

Table 4.7 clarifies the occurrence of torsional and inter-story stiffness irregularities, model D has torsional irregularity in positive Y direction since the torsional factor is greater than 1.2 where the inter-story stiffness irregularity is not existed in all lateral loads directions since the inter-story stiffness factor is less than 2 in all lateral loads directions. Torsional irregularity A1 is occurred in model D-1 because of the torsional factor in PY lateral load direction is bigger than 1.2, inter-story stiffness

irregularity B2 is not existed in both orthogonal directions since the B2 irregularity factor is less than 2. The torsional factors in both models D and D-1 are satisfies the Turkish earthquake condition to amplify the eccentricity ratios Equation 4.1 is applicable.

As shown in Table 4.8, the amplified eccentricity ratios are calculated for both models D and D-1 in accordance to equation 1, the new eccentricity ratio of model D is 0.058 in positive Y lateral load direction, however the new eccentricity ratio of model D-1 is 0.055 in positive lateral load direction.

Table 4.8: Amplified eccentricity in EPY direction of Models (D and D-1).

Model C					**Model C-1**			
Load Case	**(e)**	**η_i**	**D_i**	**A (e)**	**Load Case**	**η_i**	**D_i**	**A (e)**
EPY	0.05	1.29	1.16	0.058	**EPY**	1.26	1.1	0.055

e: Eccentricity

A: amplified

4.2.2 Reinforcement Ratios

This section compares the reinforcement ratios of columns of models that have staircase and columns of models that does not have staircase, the comparison includes only the staircase columns.

4.2.2.1 Model (A & A-1) Columns

Figure 4.9 shows the location of column C6 and column C24, steel reinforcement ratios of these two columns is compared in model A (with staircase) and model A-1 (without staircase).

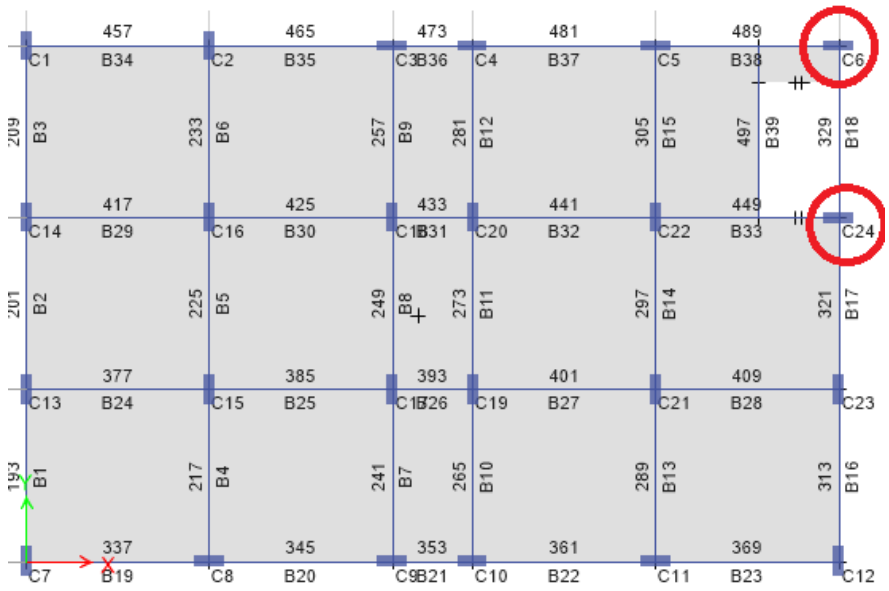

Figure 4.9: Column C6 &C24 locations in model A & A-1.

Table 4.9. Comparison of steel reinforcement ratios of column C6&C24.

	Model A	**Model A-1**	**DIFF %**
C6 (As mm²)	3521	2400	47%
C24 (As mm²)	4076	4192	-3%

Table 4.9 clarifies that required area steel of C6 in model A that contains staircase is increased by 47 % than C6 in model A-1 that does not contain staircase, for column C24 the steel area in model A is decreased by 3% than C24 in model A-1. This indicates that the staircase presence has influence on the steel reinforcement ratio of columns.

4.2.2.2 Model (B & B-1) Columns

Figure 4.10 illustrates the location of column C24 and column C23, the required area steel reinforcement of these two columns is compared in model B (with staircase) and model B-1 (without staircase).

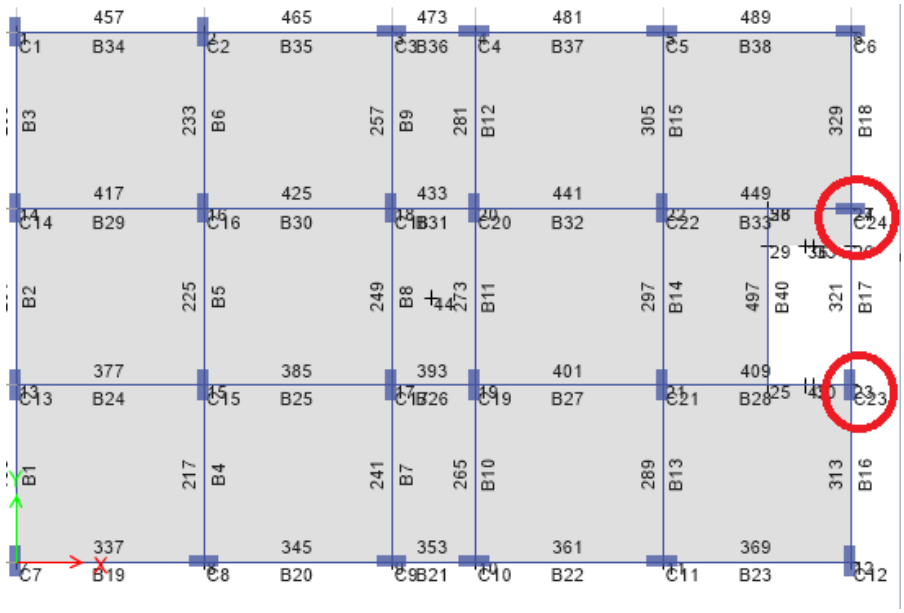

Figure 4.10: Column C24 &C23 locations in model B& B-1.

Table 4.10: Comparison of steel reinforcement ratios of column C24 & C23.

	Model B	**Model B-1**	**DIFF %**
C24 (As mm²)	3503	3286	7%
C23 (As mm²)	2400	2400	0%

Table 4.10 expounds that required area steel of C24 in model B that includes staircase is raised by 7 % than C24 in model B-1 that does not contain staircase, for column C23 the steel area in model B is the same. This denotes that area steel reinforcement is affected by staircase existence.

4.2.2.3 Model (C & C-1) Columns

Figure 4.11 represents column C18, C20, C17 and C19 locations, the steel reinforcement ratios of these columns is compared in model C (with staircase) and model C-1 (without staircase).

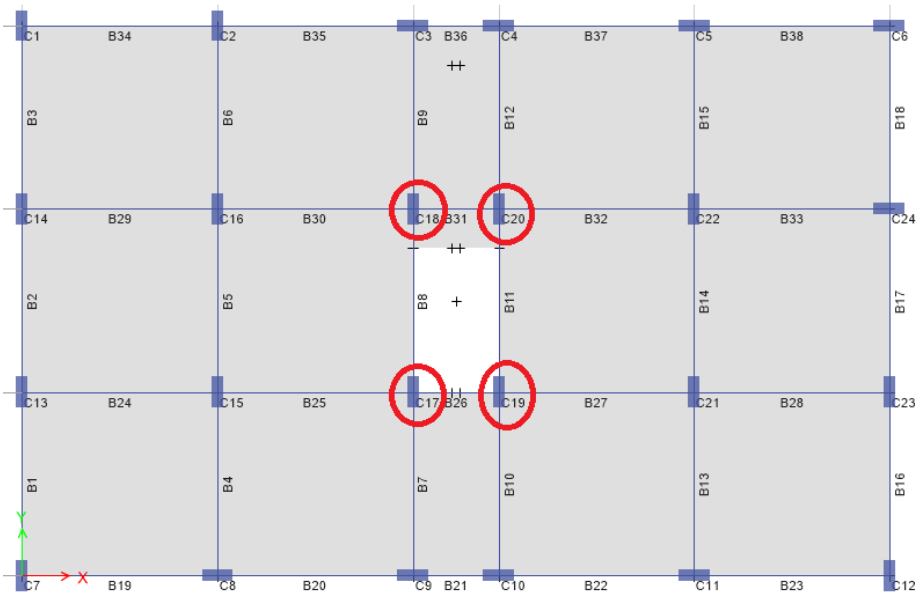

Figure 4.11: Column C18, C20, C17 and C19 locations in model C& C-1.

Table 4.11: Comparison of steel reinforcement ratios of column C18, C20, C17 and C19.

	Model C	**Model C-1**	**DIFF %**
C18 (As mm²)	3538	2400	47%
C20 (As mm²)	3475	2400	45%
C17 (As mm²)	2400	2400	0%
C19 (As mm²)	2400	2400	0%

Table 4.11 explicates that required area steel of C18 and C20 in model C that has staircase are raised by 47 and 45 and 45 % respectively than C18 and C20 in model C-1 that does not have staircase, meanwhile, column C19 and C17 steel area in model C and model C-1 is unchanged. This signifies that area steel reinforcement is influenced by staircase presence.

4.2.2.4 Model (D & D-1) Columns

Figure 4.12 shows column C18, C20, C3 and C4 locations, the steel reinforcement ratios of these columns is compared in model D (with staircase) and model D-1 (without staircase).

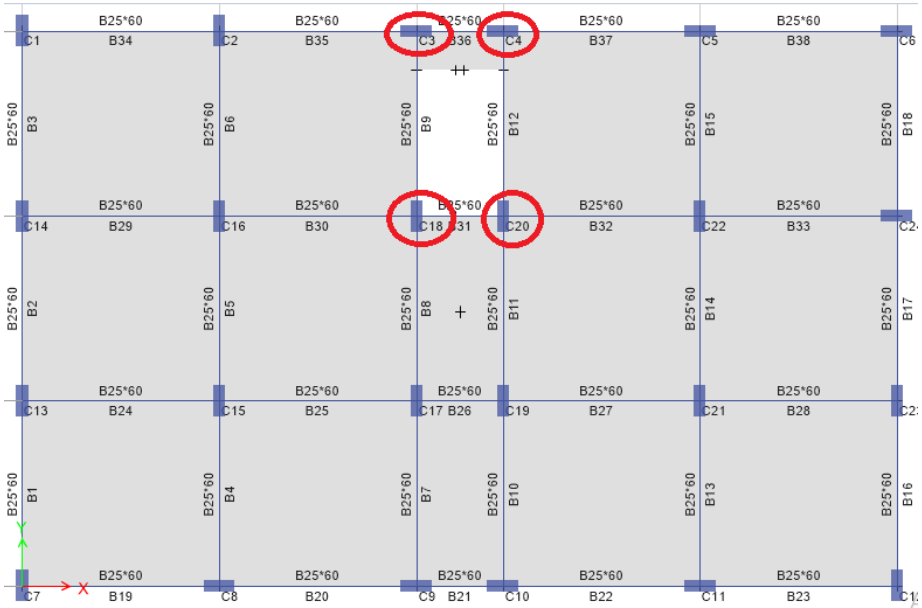

Figure 4.12: Column C18, C20, C3 and C4 locations in model D& D-1.

Table 4.12: Comparison of steel reinforcement ratios of column C18, C20, C3 and C4.

	Model D	**Model D-1**	**DIFF %**
C3 (As mm²)	3538	2400	47%
C4 (As mm²)	2465	2400	44%
C18 (As mm²)	2400	2400	0%
C20 (As mm²)	2400	2400	0%

Table 4.12 elucidates that required area steel of C3 and C4 in model D that has staircase are raised by 47 and 44 and 22 % respectively than C3 and C4 in model D-1 that does not have staircase, where column C20 and C18 steel area in model D and model D-1 is unchanged. This signifies that area steel reinforcement is influenced by the staircase existence.

4.3 Non-Linear Static Push-Over Analysis Results

A comparison between models that include staircase (model A, B, C and D) and models that do not involve staircase (model A.1, B.1, C.1 and D.1) in terms of

monitored displacements, spectral displacements, shear forces, initial stiffness and effective stiffness.

4.3.1 Hinges status

For all models with staircase and without stair case the number of plastic hinges and their phases (IO: immediate occupancy, LS: life safety, and CP: collapse prevention) in the target displacement are discussed in details in this section.

4.3.1.1 Model A & A-1

Figure 4.13(a) shows the plastic hinges status in model A in step 56 under push X lateral load case, however Figure 4.13(b) displays the status of the plastic hinges in model A at step 49 under push Y lateral load case. In both orthogonal directions the plastic hinges status is checked in the target displacement. The status of the plastic hinges of model A-1 is illustrated in Figure 4.14, (c) under push X lateral load case and (b) under push Y lateral load case. The number of the plastic hinges and their phases in both models A and A-1 are listed in Table 4.13.

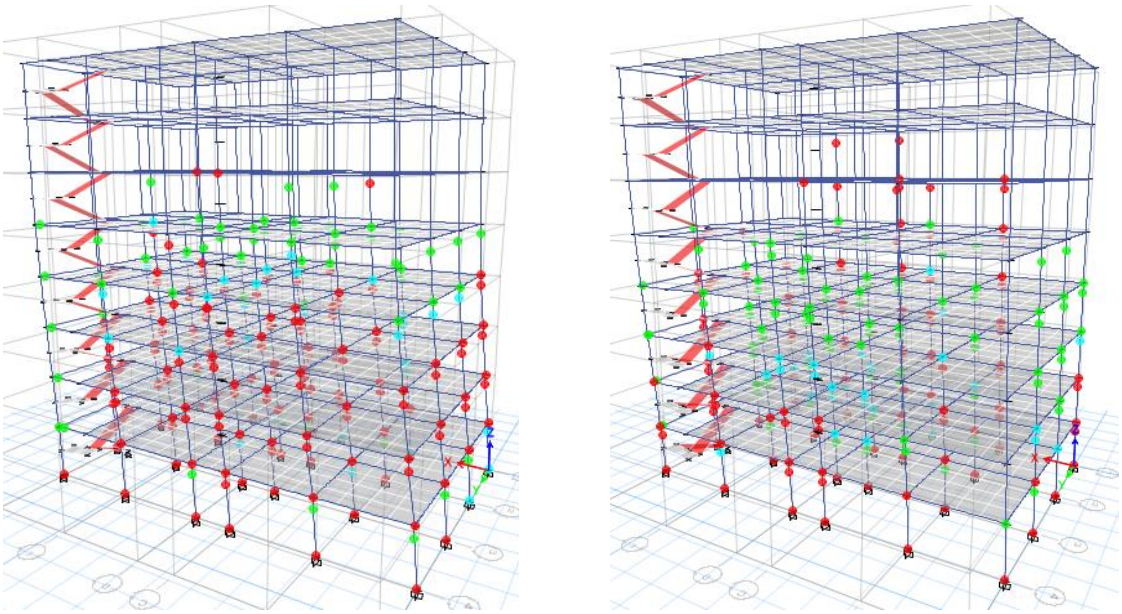

Figure 4.13: Hinges status in the structure model A at target displacement (a) load case push x, (b) load case push y.

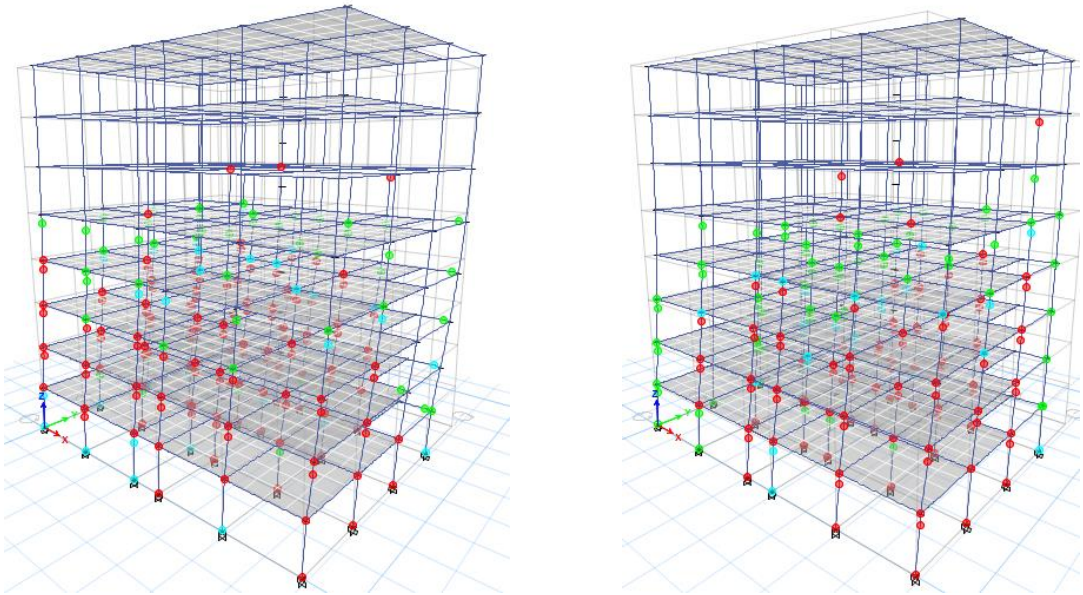

Figure 4.14: Hinges states in the structure model A-1 at target displacement (load case push x and load case push y).

Table 4.13: The total number of plastic hinges and their status in model A and model A-1.

		Model A				Model A-1			
load case	**T.N.H**	**A-IO**	**IO-LS**	**LS-CP**	**>CP**	**A-IO**	**IO-LS**	**LS-CP**	**>CP**
Push X	1008	764	61	32	151	777	54	29	148
Push Y	1008	774	91	32	111	797	65	22	124

T.N.H: Total number of hinges in the model

IO: Immediate occupancy

LF: Life safety

CP: Collapse prevention

As stated in Table 1.13, the staircase presence has an influence on the plastic hinges number and their phases, for instance the number of plastic hinges in collapse prevention phase of model A that contain staircase is greater than model A-1 that does not contain staircase under push X load case, whilst under push Y direction the plastic hinges number in collapse prevention phase of model A is less than model A-1.

4.3.1.2 Model B & B-1

The plastic hinges status at target displacement of the structure model B that contain staircase are illustrated in Figure 4.15, where (e) shows the hinges status under lateral load case push X and (f) displays the hinges status under lateral load case push Y. The Figure 4.16 demonstrates the hinges status at target displacement of the structure model B-1 that does not include staircase, (g) shows the hinges status under lateral load case push X and (h) shows the hinge the status under lateral load case push Y. the number of the plastic hinges at target displacement for both structure model B and B-1 is listed in Table 4.14.

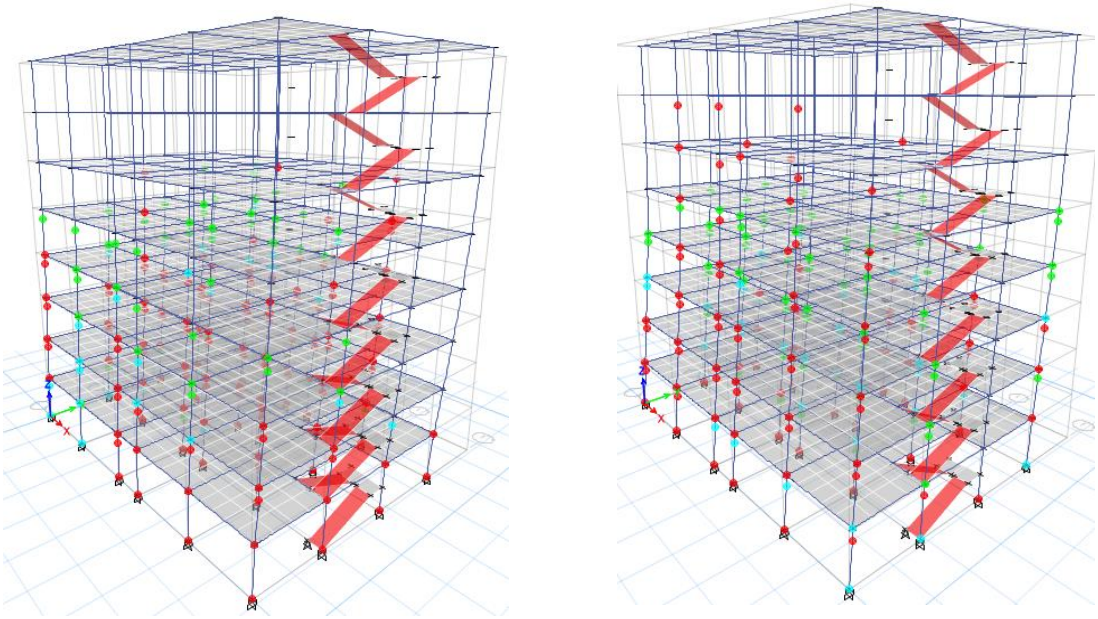

Figure 4.15: Hinges status in the structure model B at target displacement (load case push x load case push y).

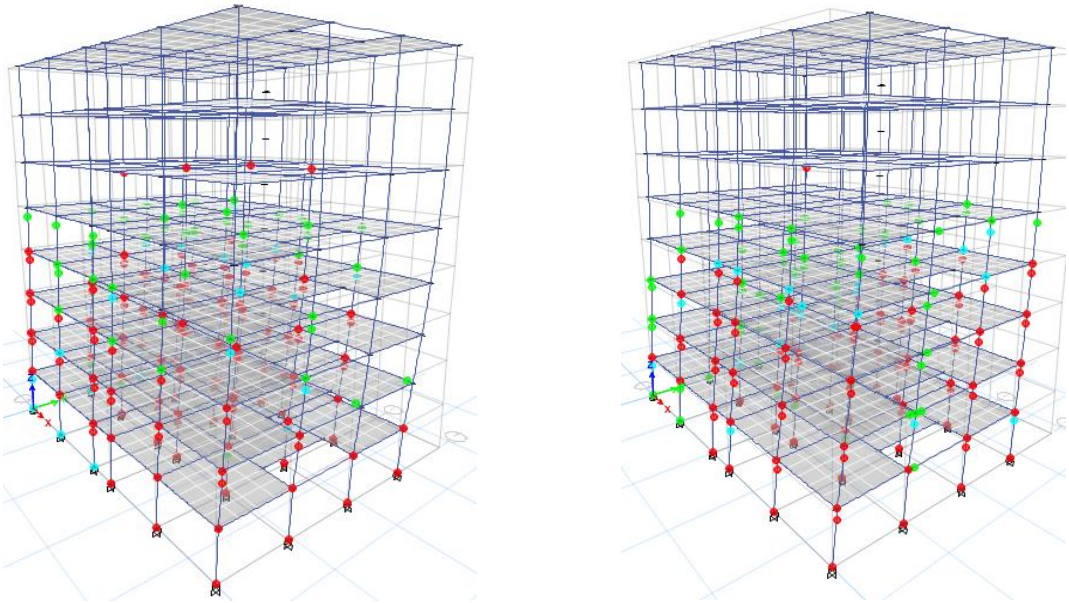

Figure 4.16: Hinges status in the structure model B-1 at target displacement (load case push x load case push y).

Table 4.14: The over-all number of plastic hinges and their status in model B and model B-1 at target displacement.

		Model B				Model B-1			
load case	**T.N.H**	**A-IO**	**IO-LS**	**LS-CP**	**>CP**	**A-IO**	**IO-LS**	**LS-CP**	**>CP**
Push X	1008	776	51	32	149	780	51	26	149
Push Y	1008	783	78	43	104	804	63	27	114

T.N.H: Total number of hinges in the model

IO: Immediate occupancy

LF: Life safety

CP: Collapse prevention

According to Table 4.14 the number of plastic hinges in collapse prevention of model B that contain staircase under push X load case is the same number of plastic hinges in collapse prevention of model B-1 that does not involve staircase, while under push Y lateral load case the collapse prevention hinges of model B are smaller than model B-1, this indicates that the staircase influence the behaviour of the structure members under lateral loads.

4.3.1.2 Model C & C-1

Figure 4.17 displays the plastic hinges phases of model C (with staircase) under both lateral load orthogonal directions at target displacement, (i) presents the hinges phases under push X load case and (j) demonstrates the hinges phases under push Y load case. Figure 4.18 illustrates the plastic hinges phases of model C.1 (without staircase) in both lateral load directions at target displacement, where (k) and (l) show the hinges phases under lateral load case push X and push Y respectively. The total number of plastic hinges and their phases is listed in Table 4.15.

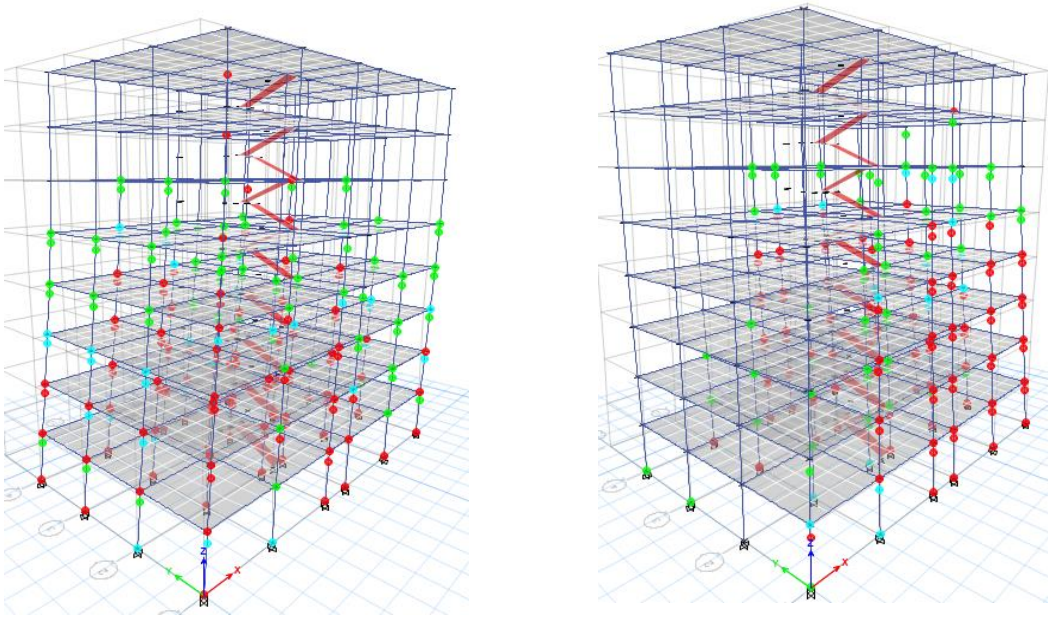

Figure 4.17: Hinges status in the structure model C at target displacement (load case push x and load case push y.

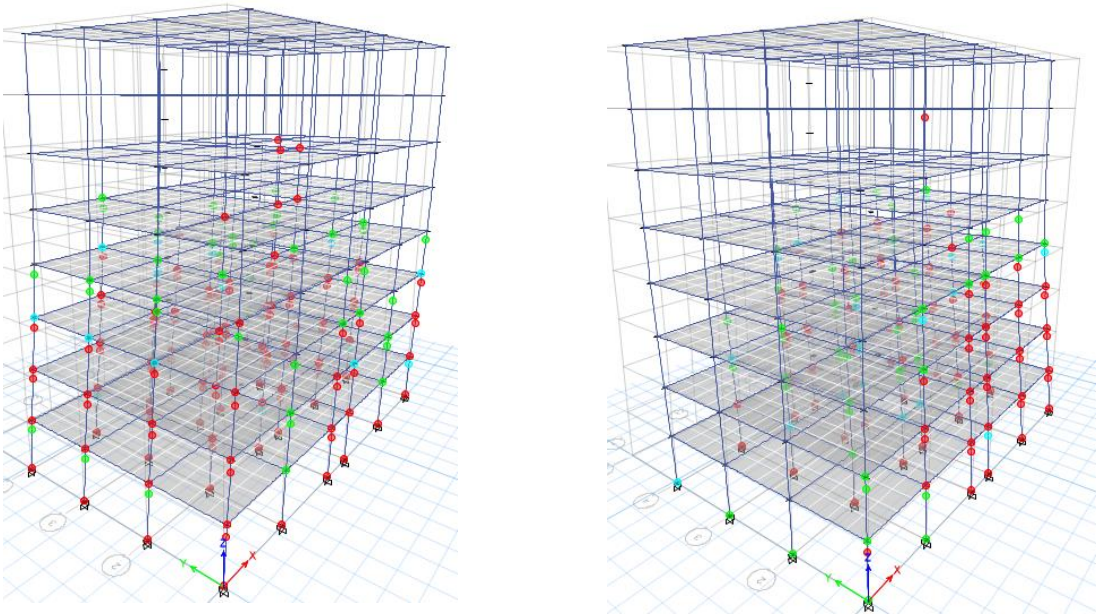

Figure 4.18: Hinges status in the structure model C-1 at target displacement (load case push x load case push y).

Table 4.15: The total number of plastic hinges and their status in model C and model C-1 at target displacement.

		Model C				Model C-1			
load case	**T.N.H**	**A-IO**	**IO-LS**	**LS-CP**	**>CP**	**A-IO**	**IO-LS**	**LS-CP**	**>CP**
Push X	992	749	82	37	124	789	47	16	140
Push Y	992	786	61	22	123	823	55	12	102

T.N.H: Total number of hinges in the model

IO: Immediate occupancy

LF: Life safety

CP: Collapse prevention

The total plastic hinges and their phases at target displacement are provided in Table 4.15, the number of plastic hinges in collapse prevention phase under push X load case of model C that contain staircase is smaller than of model C-1 that does not involve staircase, whilst collapse prevention hinges number under push Y in model C is greater than model C-1. It is observed that the staircase affect the reaction of structure elements under lateral load application.

4.3.1.2 Model D& D-1

The plastic hinges phases at target displacement for model D that include staircase and model D-1 that does not include staircase are displayed at Figure 4.19-4.0 under both lateral load cases push X and push Y respectively, in addition to that the total number of hinges and their phases for models are listed in Table 16.

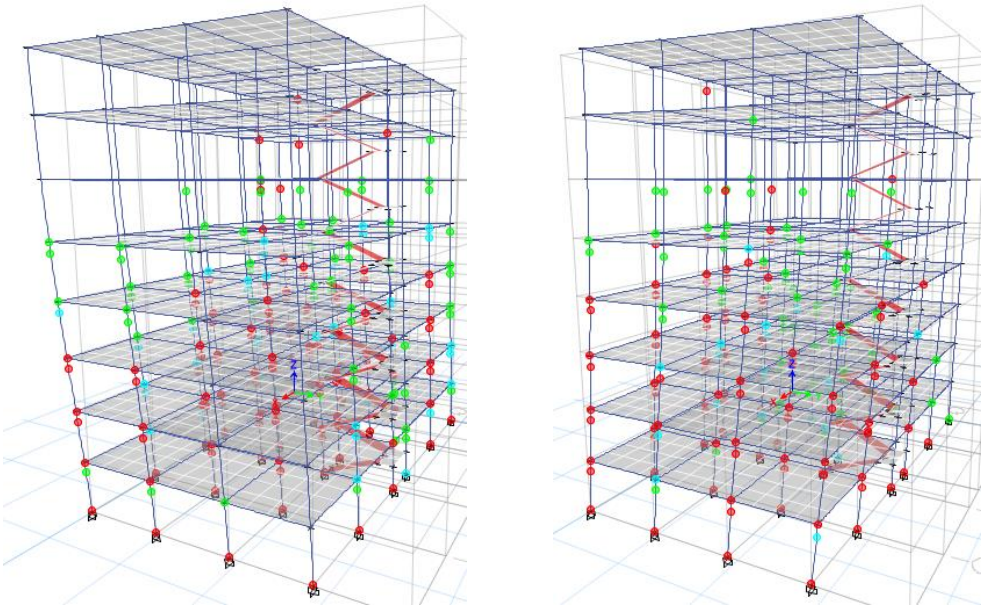

Figure 4.19: Hinges status in the structure model D at target displacement (load case push x and load case push y).

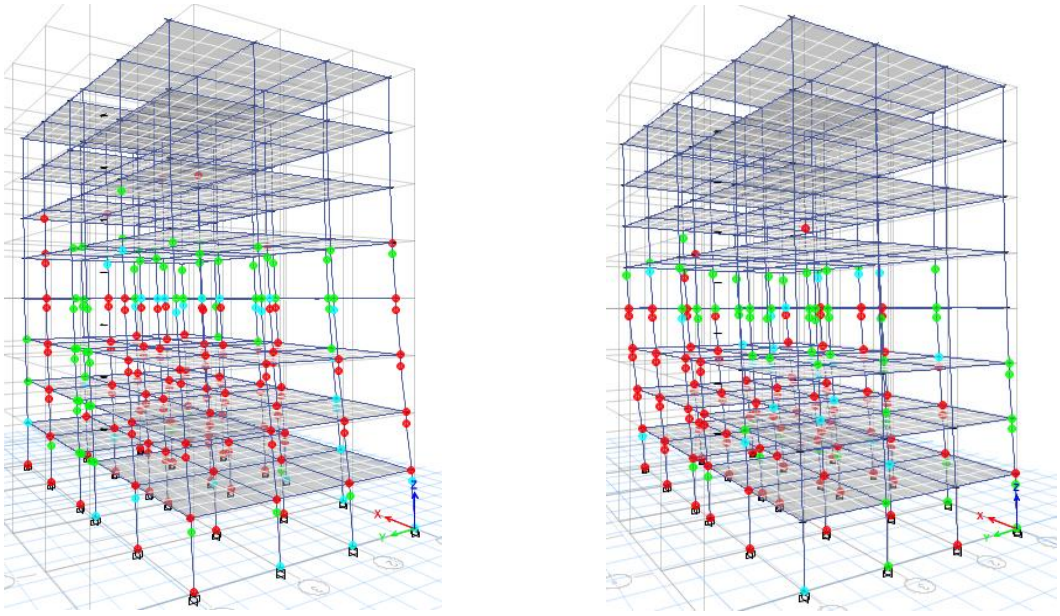

Figure 4.20: Hinges status in the structure model D-1 at target displacement (load case push x and load case push y).

Table 4.16: The over-all number of plastic hinges and their status in model D and model D-1 at target displacement.

		Model D				Model D-1			
load case	**T.N.H**	**A-IO**	**IO-LS**	**LS-CP**	**>CP**	**A-IO**	**IO-LS**	**LS-CP**	**>CP**
Push X	992	749	75	39	129	749	71	31	141
Push Y	992	791	73	23	105	789	60	23	120

T.N.H: Total number of hinges in the model

IO: Immediate occupancy

LF: Life safety

CP: Collapse prevention

As shown in Table 4.16, the number of plastic hinges at collapse prevention phase at target displacement of model D (with staircase) is smaller than model D-1 (without staircase) under both lateral load case push X and push Y. it is obtained that the presence of staircase affects the structure beams and columns behaviour under lateral applied loads.

4.3.1 Monitored Displacement

Displacements of models that contain staircase and models that do not contain staircase are compared at performance point of the models.

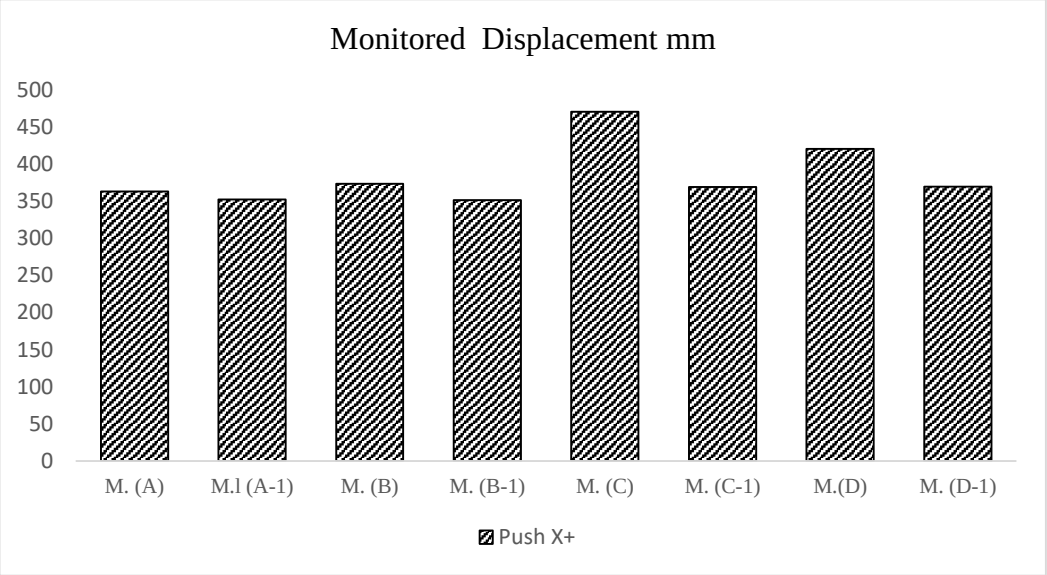

Figure 4.21: Monitored displacements of all models in push-X positive.

Figure 4.21 displays the monitored displacements at the performance point of all models with and without staircase in push X+. In model A, B, C and D that include staircase the monitored displacements were larger than in model A.1, B.1, C.1 and D.1 that does not include staircase by 3%, 6%, 27% and 14% respectively. This indicates that monitored displacements increased in push X+ by considering staircase in building design.

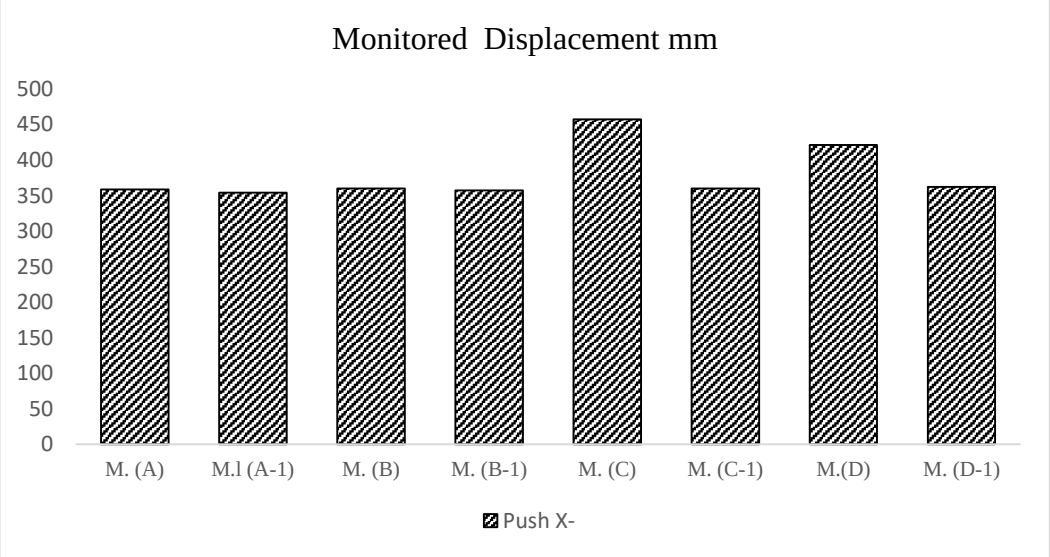

Figure 4.22: Monitored displacements of all models in push-X negative.

Figure 4.22 illustrates the monitored displacements at the performance point of all models with and without staircase in push X-. In model A, B, C and D that contain staircase the monitored displacements were larger than in model A.1, B.1, C.1 and D.1 that does not contain staircase by 1%, 1%, 27% and 16% respectively. It is observed that monitored displacements augmented in push X- when including staircase in building design.

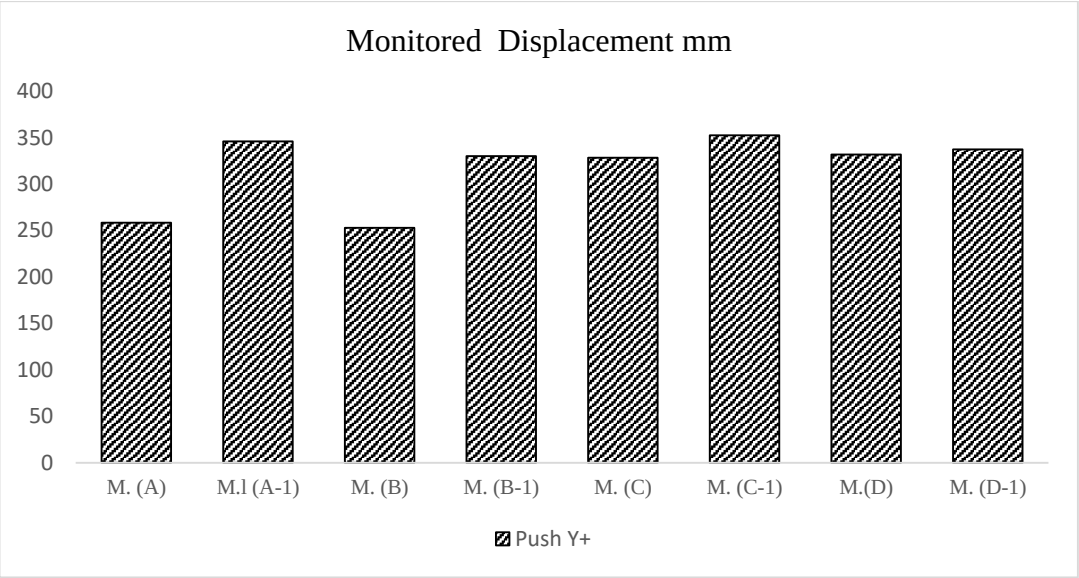

Figure 4.23: Monitored displacements of all models in push-Y positive.

Figure 4.23 shows the monitored displacements at the performance point of all models with and without staircase in push Y+. In model A, B, C and D that contain staircase the monitored displacements were smaller than in model A.1, B.1, C.1 and D.1 that does not contain staircase by 25%, 23%, 7% and 2% respectively. It is observed that monitored displacements is reduced by including staircase in the models in push Y+.

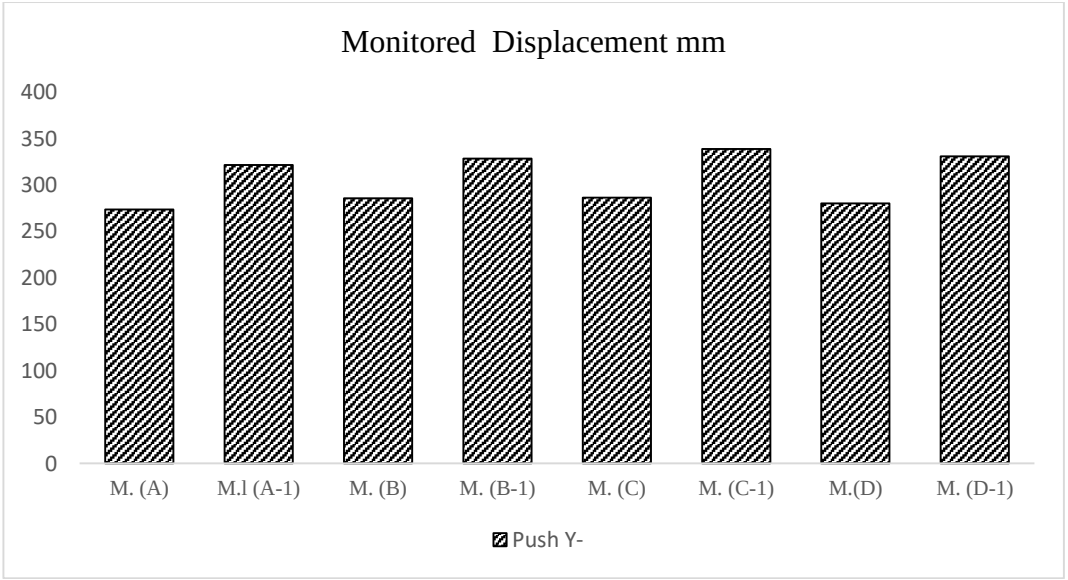

Figure 4.24: Monitored displacements of all models in push-Y negative.

Figure 4.24 clarifies the monitored displacements at the performance point of all models with and without staircase in push Y-. In model (A), (B), (C) and (D) that contain staircase the monitored displacements were smaller than in model A.1, B.1, C.1 and D.1 that does not contain staircase by 15%, 13%, 15% and 15% respectively. It is obtained that monitored displacements is decreased by containing staircase in the models in push Y.

4.3.2 Spectral Displacement

Spectral displacements of models that include staircase and models that do not contain staircase are compared at performance point of the models.

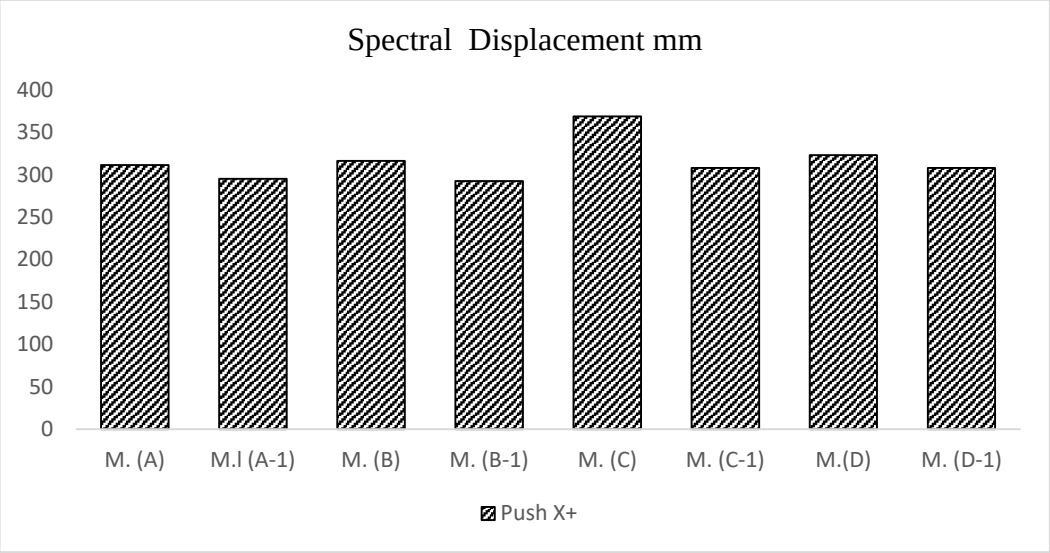

Figure 4.25: Spectral displacements of all models in push-X positive.

Figure 4.25 illustrates the spectral displacements at the performance point of all models with and without staircase in push X+. In model (A), (B), C and D that include staircase, the spectral displacements were larger than in model A.1, B.1, C.1 and D.1 that does not include staircase by 5%, 8%, 20% and 5% respectively. It is found that spectral displacements raised in push X+ by including staircase in building design.

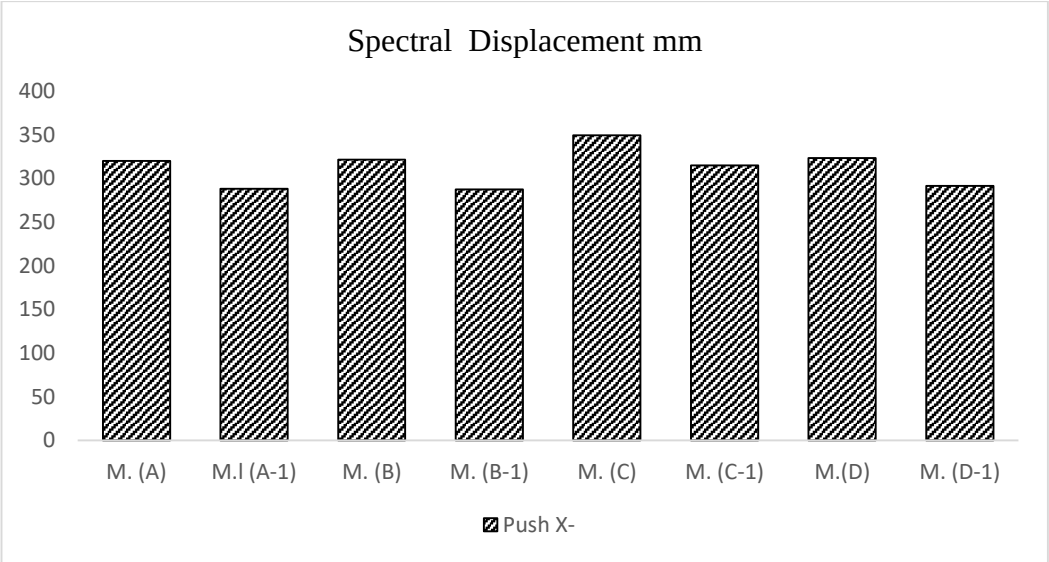

Figure 4.26: Spectral displacements of all models in push-X negative.

Figure 4.26 demonstrates the spectral displacements at the performance point of all models with and without staircase in push X-. In model A, B, C and D that contain staircase, the spectral displacements were larger than in model A.1, B.1, C.1 and D.1 that does not contain staircase by 11%, 12%, 17% and 11% respectively. It is disclosed that spectral displacements augmented in push X- when considering staircase in building design.

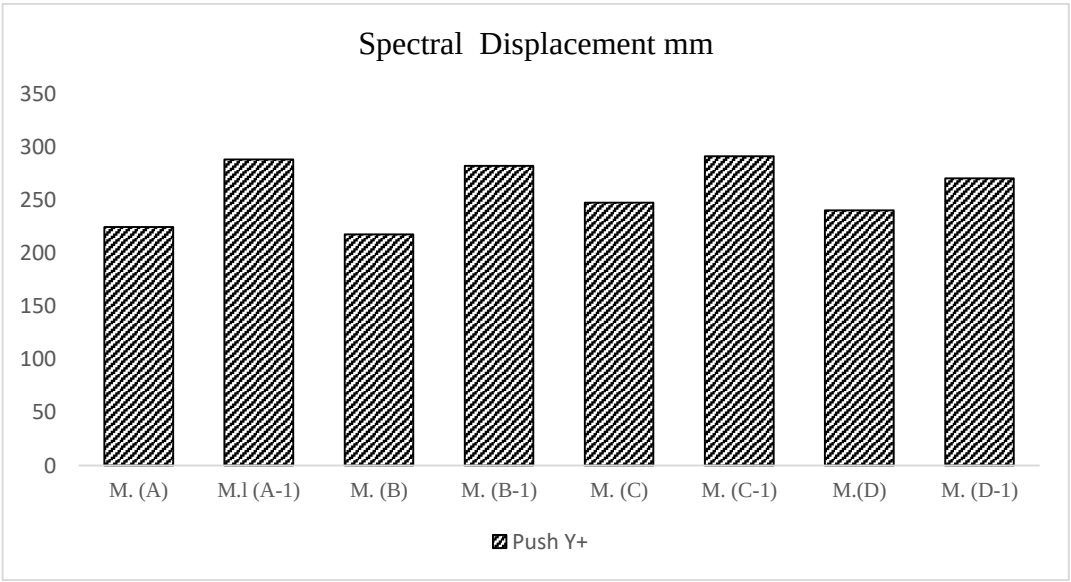

Figure 4.27: Spectral displacements of all models in push-Y positive.

Figure 4.27 shows the spectral displacements at the performance point of all models with and without staircase in push Y+. In model (A), (B), (C) and (D) that contain staircase, the spectral displacements were smaller than in model A.1, B.1, C.1 and D.1 that do not comprise staircase by 22%, 23%, 15% and 11% respectively. It is acquired that spectral displacements is reduced by comprising staircase in the models in push Y+.

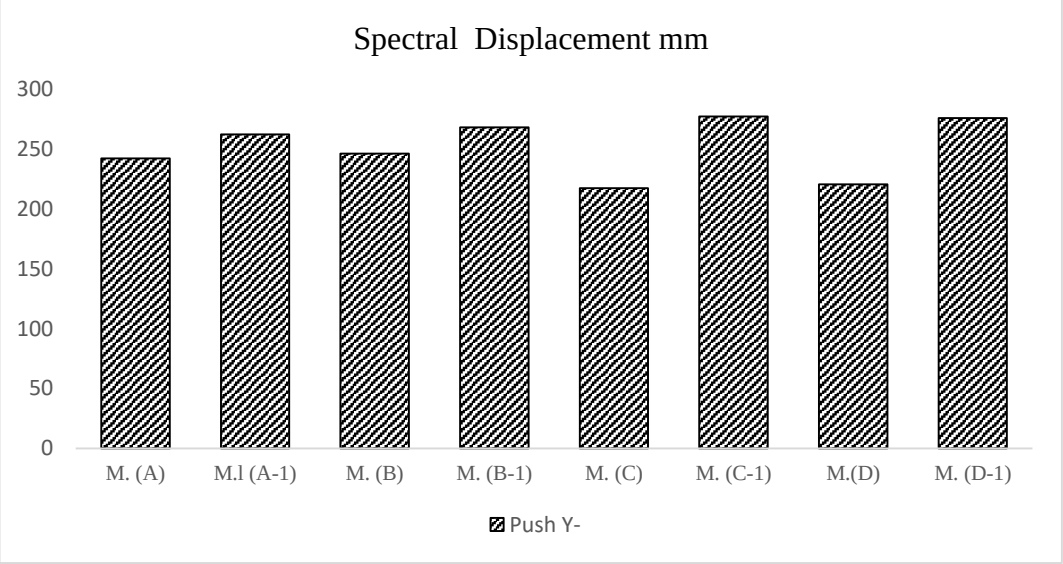

Figure 4.28: Spectral displacements of all models in push-Y negative.

Figure 4.28 clarifies the spectral displacements at the performance point of all models with and without staircase in push Y-. In model (A), (B), (C) and (D) that contain staircase the spectral displacements were smaller than in model A.1, B.1, C.1 and D.1 that do not contain staircase by 8%, 8%, 22% and 20% respectively. It is observed that spectral displacements is decreased by including staircase in the models in push Y.

4.3.3 Shear Force

Shear forces of models that contain staircase and models that do not comprise staircase are compared at performance point of the models.

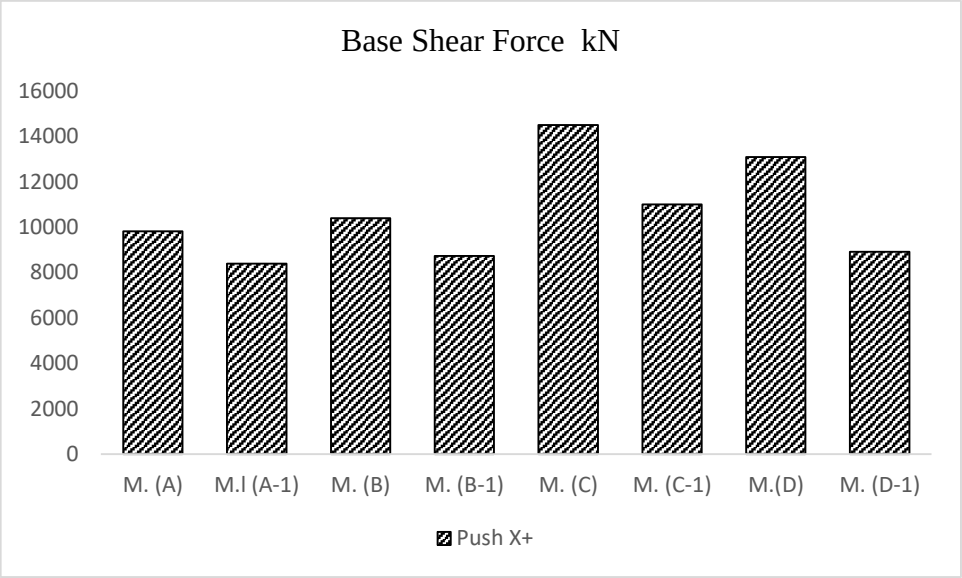

Figure 4.29: Shear forces of all models in push-X positive.

Figure 4.29 illustrates the shear forces at the performance point of all models with and without staircase in push X+. In model A, B, C and D that include staircase, the shear forces were larger than in model A.1, B.1, C.1 and D.1 that do not comprise staircase by 17%, 19%, 32% and 47% respectively. It is obtained that shear forces of models that contain staircase are increased in push X+.

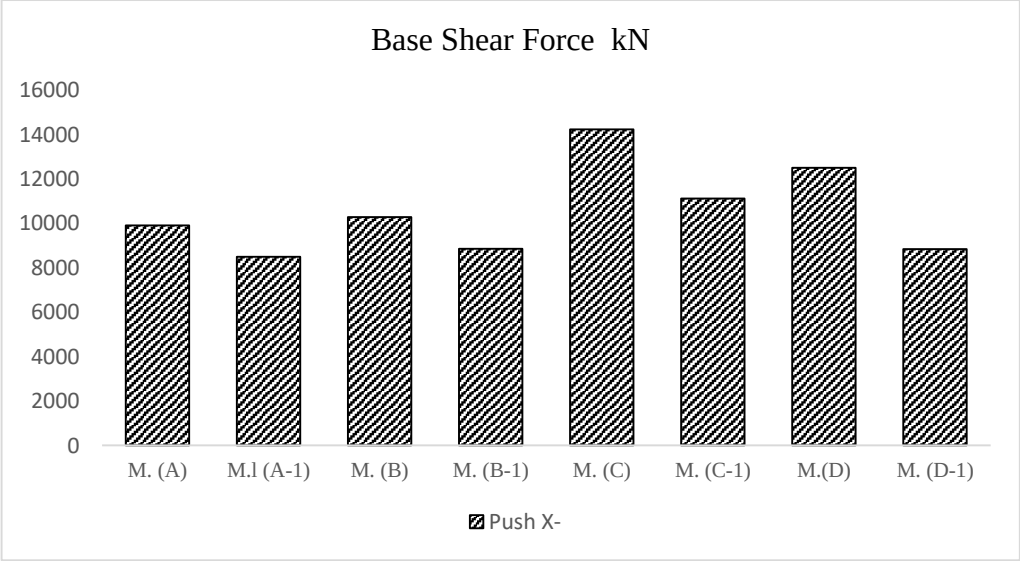

Figure 4.30: Shear forces of all models in push-X negative.

Figure 4.30 displays the shear forces at the performance point of all models with and without staircase in push X negative. In model A, B, C and D that include staircase, the shear forces were larger than in model A.1, B.1, C.1 and D.1 that do not contain staircase by 17%, 16%, 36% and 41% respectively. It is attained that the existence of staircase has influence on shear forces in push X-.

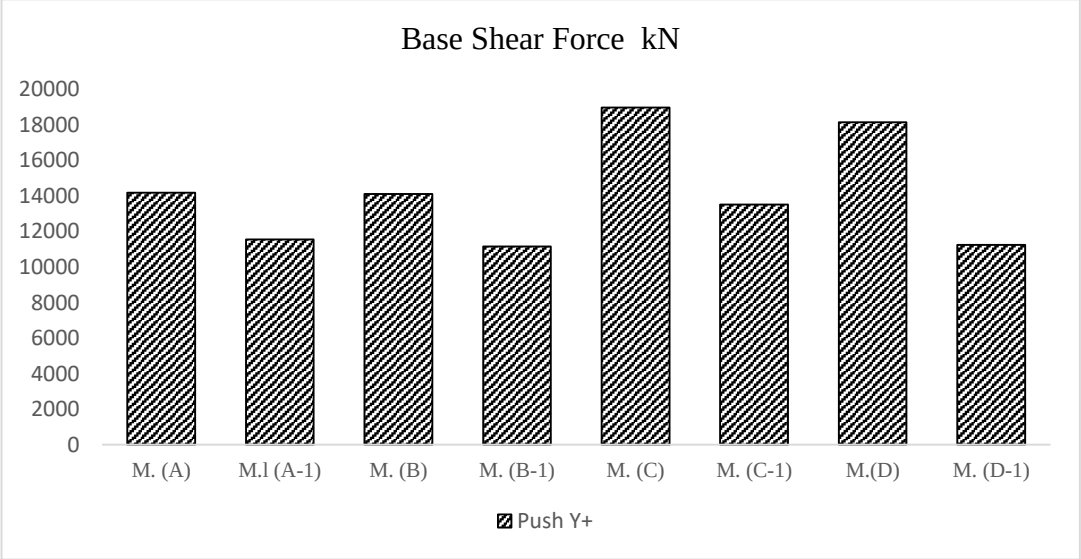

Figure 4.31: Shear forces of all models in push-Y positive.

Figure 4.31 presents the shear forces at the performance point of all models with and without staircase in push Y+. In model (A), (B), (C) and (D) that comprise staircase, the shear forces were larger than in model A.1, B.1, C.1 and D.1 that do not comprise staircase by 23%, 26%, 40% and 61% respectively. It is noticed that the presence of staircase has affected the shear forces in push Y+.

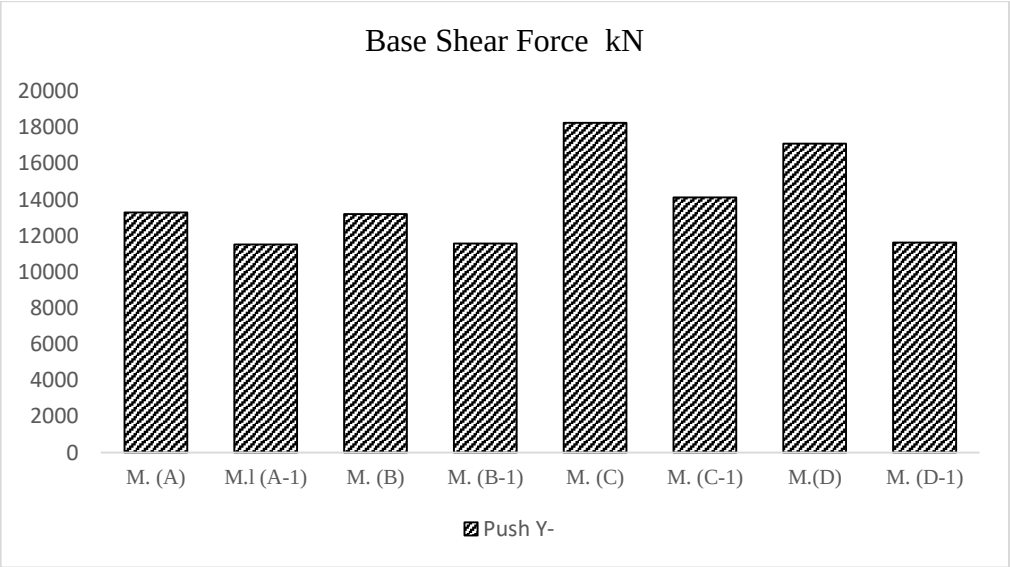

Figure 4.32: Shear forces of all models in push-Y negative.

Figure 4.32 illustrates the shear forces at the performance point of all models with and without staircase in push Y negative. In model A, B, C and D that contain staircase, the shear forces were larger than in model A.1, B.1, C.1 and D.1 that do not contain staircase by 15%,14%, 29% and 47% respectively. This indicates that the staircase has an impact on shear force of the building in push Y negative.

4.3.4 Initial Lateral Stiffness

Initial lateral stiffness of models that involve staircase and models that do not involve staircase are compared at performance point of the models.

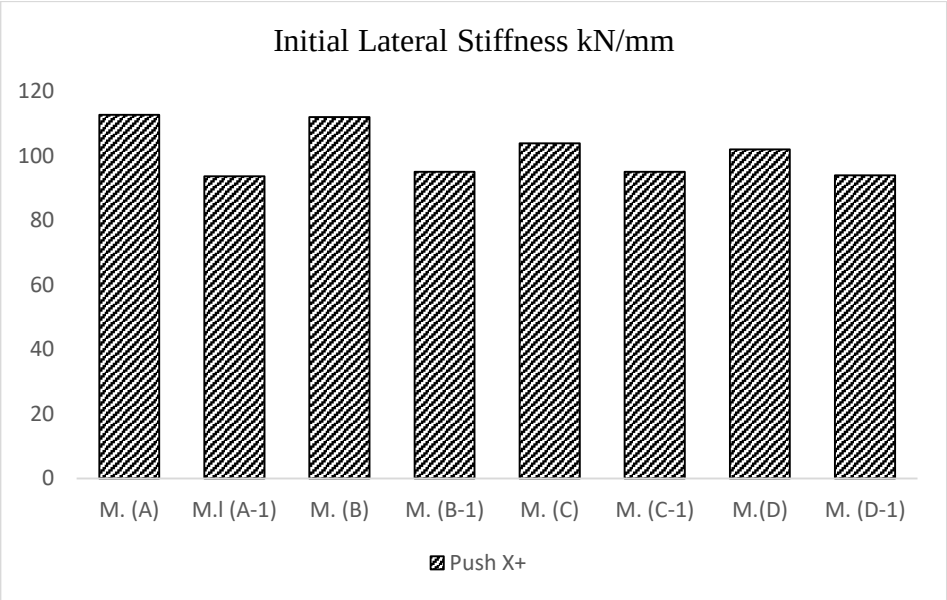

Figure 4.33: Initial lateral stiffness of all models in push X+.

Figure 4.33 displays initial lateral stiffness at the performance point of all models with and without staircase in push X positive. In model A, B, C and D that include staircase, initial lateral stiffness was larger than in model A-1, B-1, C-1 and D-1 that do not include staircase by 20%, 18%, 9% and 8% respectively. It is attained that the existence of staircase has influence on initial lateral stiffness in push X+.

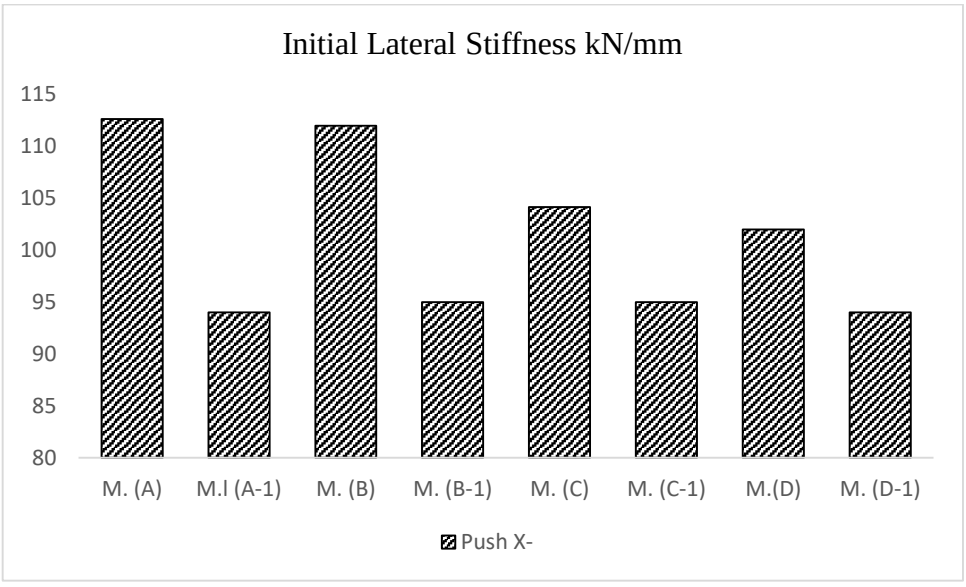

Figure 4.34: Initial lateral stiffness of all models in push X-.

Figure 4.34 shows the initial lateral stiffness at the performance point of all models with and without staircase in push X negative. In model A, B, C and D that contain staircase, the initial lateral stiffness was larger than in model A.1, B.1, C.1 and D.1 that do not contain staircase by 20%, 18%, 10% and 9% respectively. It is acquired that the initial lateral stiffness is influenced by the existence of the staircase in push X-.

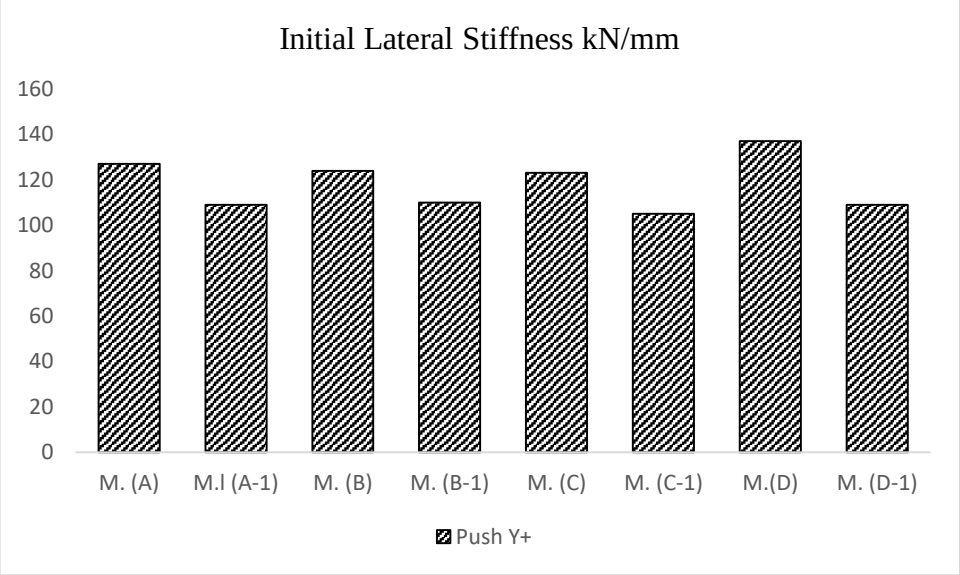

Figure 4.35: Initial lateral stiffness of all models in push Y+.

Figure 4.35 illustrates the initial lateral stiffness at the performance point of all models with and without staircase in push Y+. In model A, B, C and D that involve staircase, the initial lateral stiffness was larger than in model A.1, B.1, C.1 and D.1 that do not involve staircase by 17%, 13%, 17% and 26% respectively. It is attained that the initial lateral stiffness is affected by the presence of the staircase in push Y+.

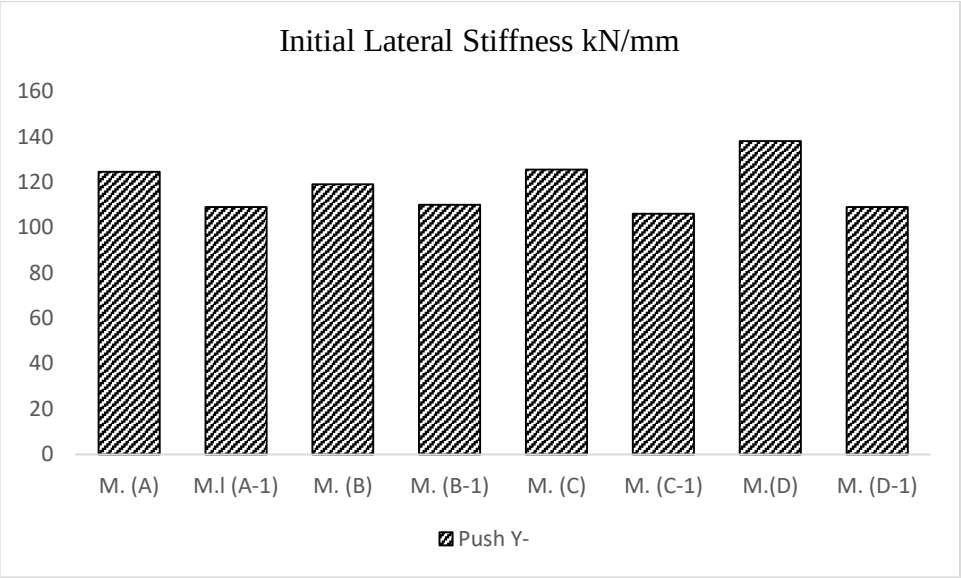

Figure 4.36: Initial lateral stiffness of all models in push Y-.

Figure 4.36 demonstrates the initial lateral stiffness at the performance point of all models with and without staircase in push Y-. In model A, B, C and D that comprise staircase, the initial lateral stiffness was larger than in model A.1, B.1, C.1 and D.1 that do not comprise staircase by 14%, 8%, 14% and 27% respectively. It is observed that the presence of the staircase has an impact on the initial lateral stiffness in push Y-.

4.3.5 Effective Lateral Stiffness

Effective lateral stiffness of models that include staircase and models that do not include staircase are compared at performance point of the models.

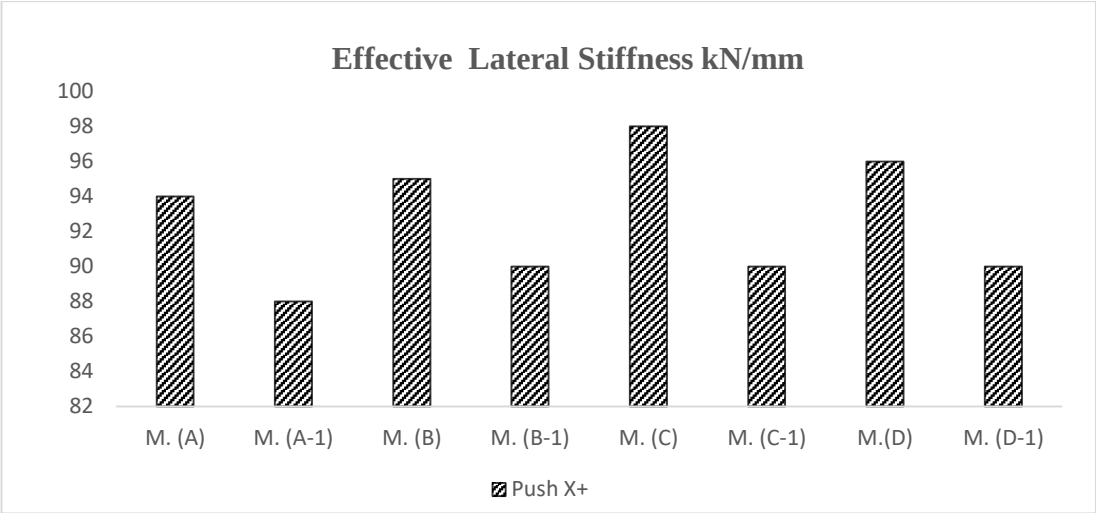

Figure 4.37: Effective lateral stiffness of all models in push X+.

Figure 4.37 displays effective lateral stiffness at the performance point of all models with and without staircase in push X+. In model A, B, C and D that include staircase, effective lateral stiffness was larger than in model A.1, B.1, C.1 and D.1 that do not include staircase by 7%, 6%, 9% and 7% respectively. This indicates that the existence of staircase affects the initial lateral stiffness in push X+.

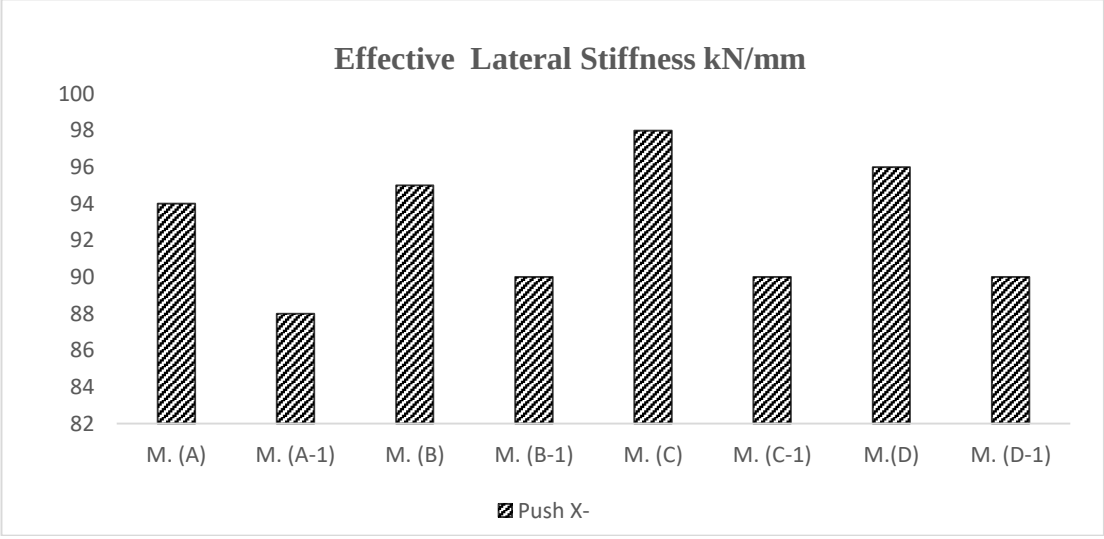

Figure 4.38: Effective lateral stiffness of all models in push X-.

Figure 4.38 presents the initial lateral stiffness at the performance point of all models with and without staircase in push X negative. In model A, B, C and D that contain staircase, the effective lateral stiffness was larger than in model A.1, B.1, C.1 and

D.1 that do not contain staircase by 7%, 6%, 9% and 7% respectively. It is observed that the effective lateral stiffness is increased by the existence of the staircase in push X-.

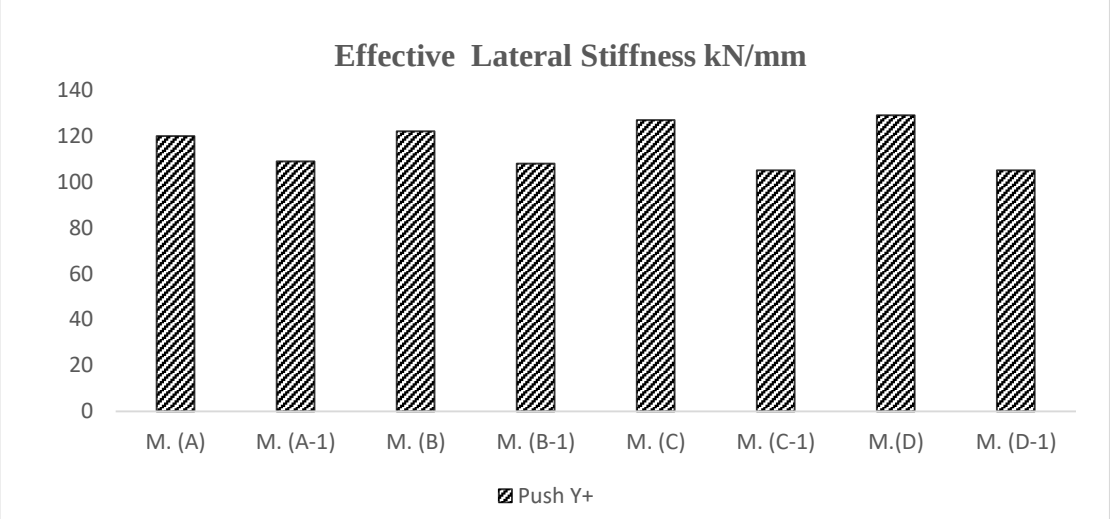

Figure 4.39: Effective lateral stiffness of all models in push Y+.

Figure 4.39 shows the effective lateral stiffness at the performance point of all models with and without staircase in push Y+. In model A, B, C and D that involve staircase, the effective lateral stiffness was larger than in model A.1, B.1, C.1 and D.1 that do not involve staircase by 10%, 13%, 21% and 23% respectively. It is attained that the effective lateral stiffness is augmented by the presence of the staircase in push Y+.

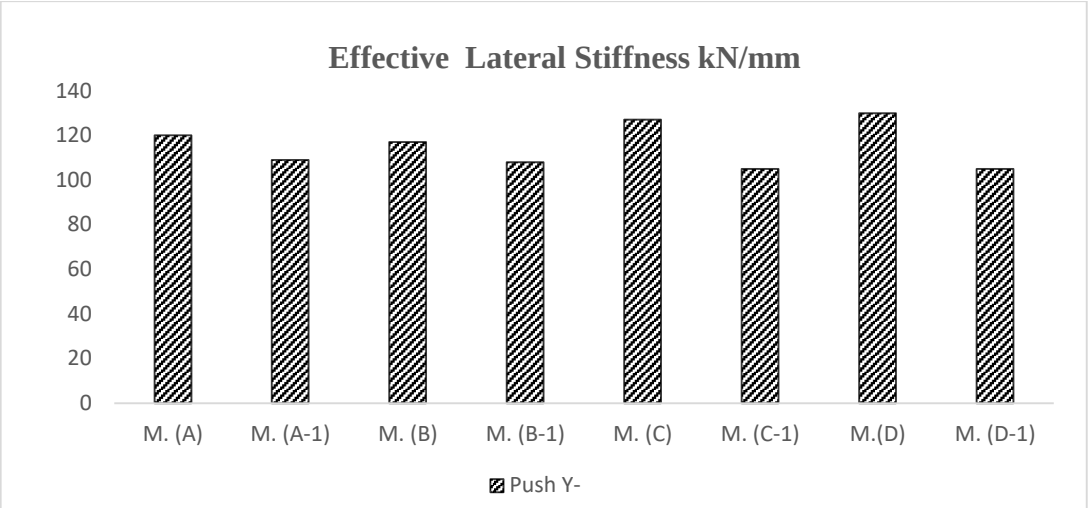

Figure 4.40: Effective lateral stiffness of all models in push Y-.

Figure 4.40 displays the effective lateral stiffness at the performance point of all models with and without staircase in push Y-. In model A, B, C and D that comprise staircase, the effective lateral stiffness was larger than in model A.1, B.1, C.1 and D.1 that do not comprise staircase by 14%, 8%, 14% and 27% respectively. It is observed that the initial lateral stiffness increased by presence of the staircase in push Y-.

4.4 Time History Analysis Results

It was found that Duzce earthquake has the biggest effects on the structural models, therefore its results will be discussed. A comparison between models that include staircase (model A, B, C and D) and models that do not involve staircase (A.1, B.1, C.1 and D.1) in terms of displacements, maximum drift, shear force and formation of plastic hinges. The formation of short columns is also discussed in this section.

4.4.1 Displacement

Diaphragm center of mass displacements of models that include staircase and models that do not include staircase are compared.

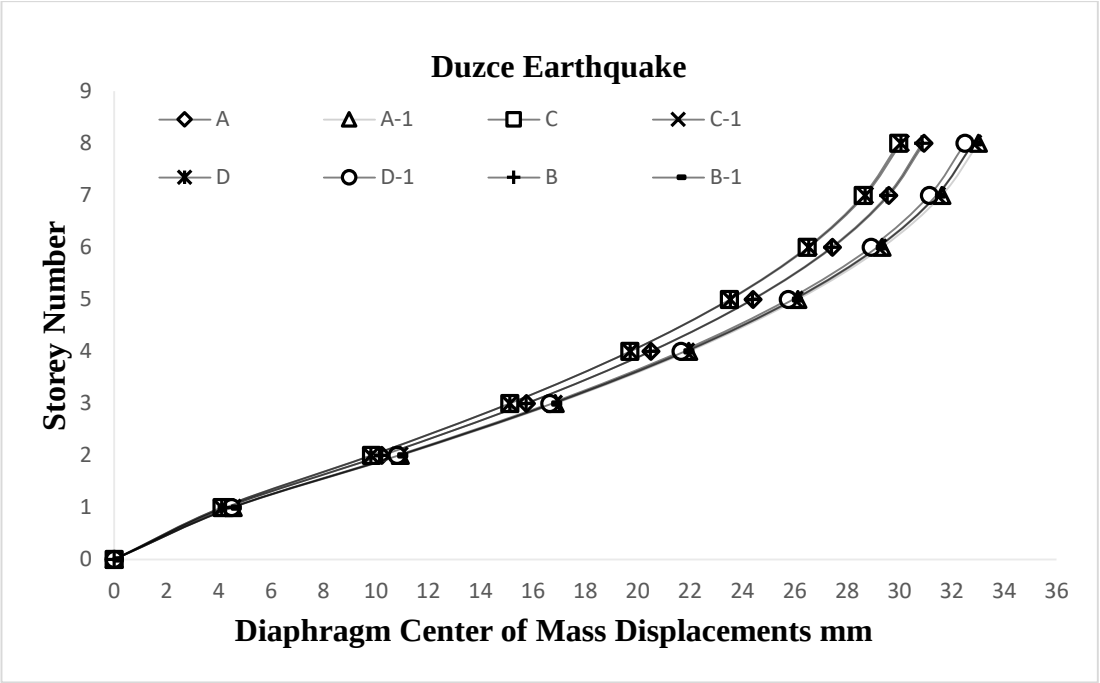

Figure 4.41: Displacement under non-linear dynamic time history load case is in X direction.

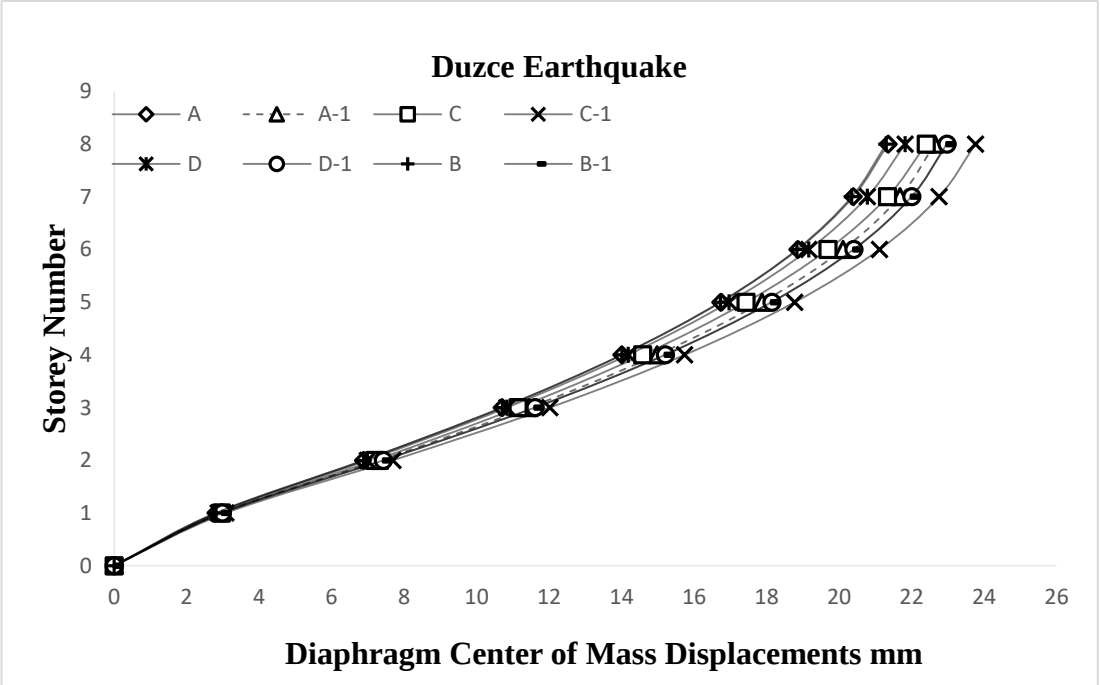

Figure 4.42: Displacement under non-linear dynamic time history load case is in Y direction.

As shown in Figure 4.41 and 4.42, the staircase presence and its location has no significant influence on the diaphragm center of mass displacements in both orthogonal directions. However, the maximum displacement in X direction was 33.1

mm in Model A-1 and the minimum displacement in X direction was 30 mm in Model C. the maximum displacement in Y direction was 23.8 mm in Model C-1 and the minimum displacement in Y direction was 21.3 mm in Model B.

4.4.2 Max Storey Drift

Max drift of models that involve staircase and models that do not contain staircase are compared at time 27s of Duzce earthquake.

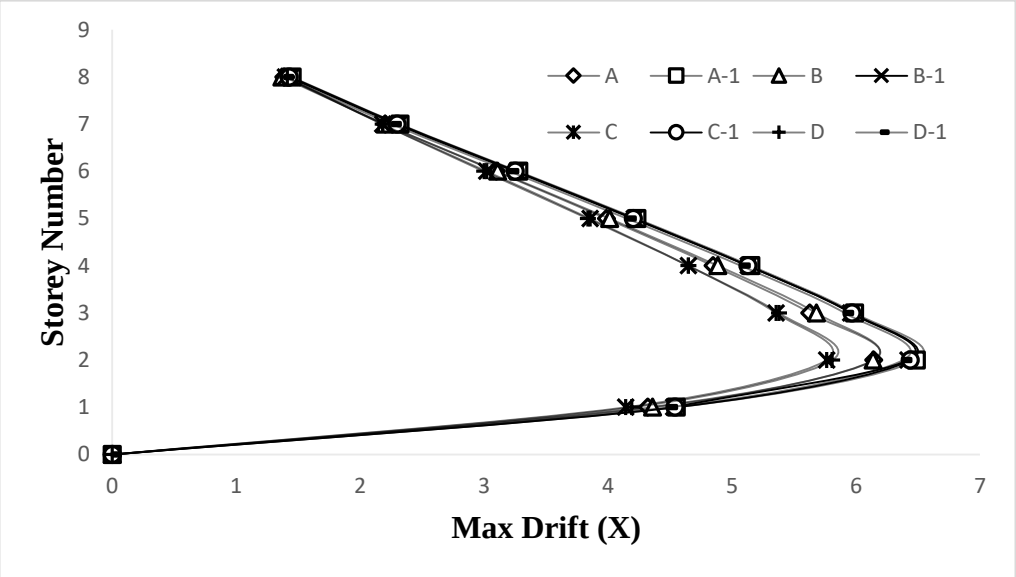

Figure 4.43: Max storey drift under non-linear dynamic time history load case is in X direction.

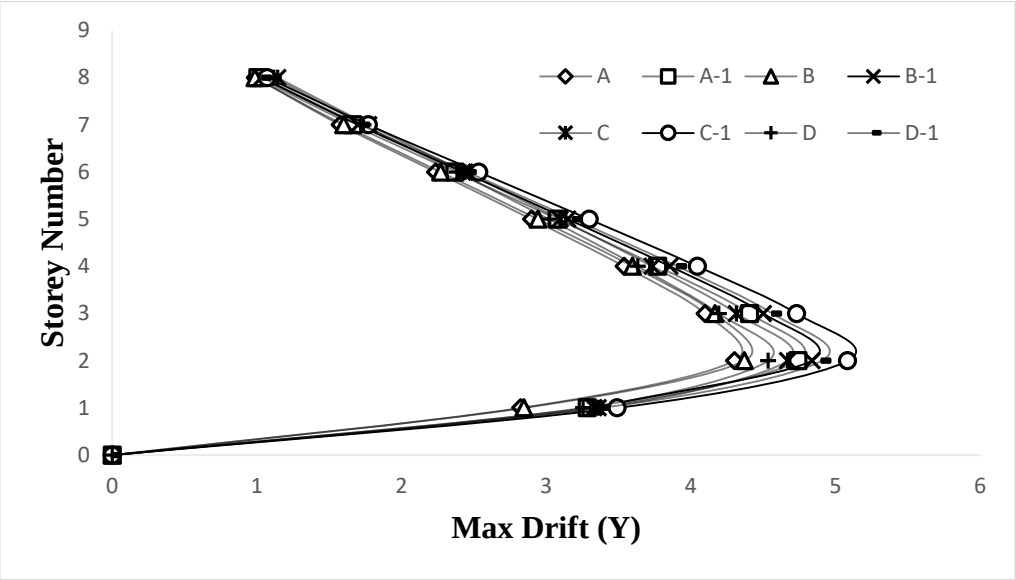

Figure 4.44: Max storey drift under non-linear dynamic time history load case is in Y direction.

As shown in Figure 4.43 and 4.44, the staircase presence and its location has no significant influence on the max drift in both orthogonal directions. The maximum storey drift in X direction was 1.45 mm in Model A-1 and the minimum storey drift in X direction was 1.397 mm in Model C. The maximum storey drift in Y direction was 1.072 mm in Model C-1 and the minimum displacement in Y direction was 0.988 mm in Model B.

4.4.3 Formation of Collapse Prevention Plastic Hinges

Table show the formation of collapse prevention plastic hinges of all models at time 27s of Duzce earthquake in both load cases which are non-linear dynamic time history in X direction and non-linear dynamic time history in Y direction.

Table 4.17: Formation of collapse prevention plastic hinges in all Models.

	Duzce Earthquake	
	Collapse prevention hinges (X)	**Collapse prevention hinges (Y)**
Model A	18	2
Model A-1	11	1
Model B	14	3
Model B-1	12	1
Model C	7	3
Model C-1	11	1
Model D	9	5
Model D-1	7	1

According to Table 4.17, the maximum occurrence of collapse hinges was in Model A 18 hinges under load in X direction and 2 hinges under load in Y direction. The minimum formation of collapse hinges was 7 hinges under load in X direction and 1 hinge under load in Y direction in Model D-1. It was observed in all models (that contain staircase) that the formation of collapse hinges was significantly smaller in Y direction (staircase direction) than in X direction. This indicates that the staircase location and its presence has influenced the formation of collapse plastic hinges.

4.4.3 Formation of Short Columns

The formation of short columns is due to additional shear forces is applied on staircase columns which carry the land slab. Shear forces of columns which carry the land slab of the staircase are displayed in Figure 4.45 to 4.48.

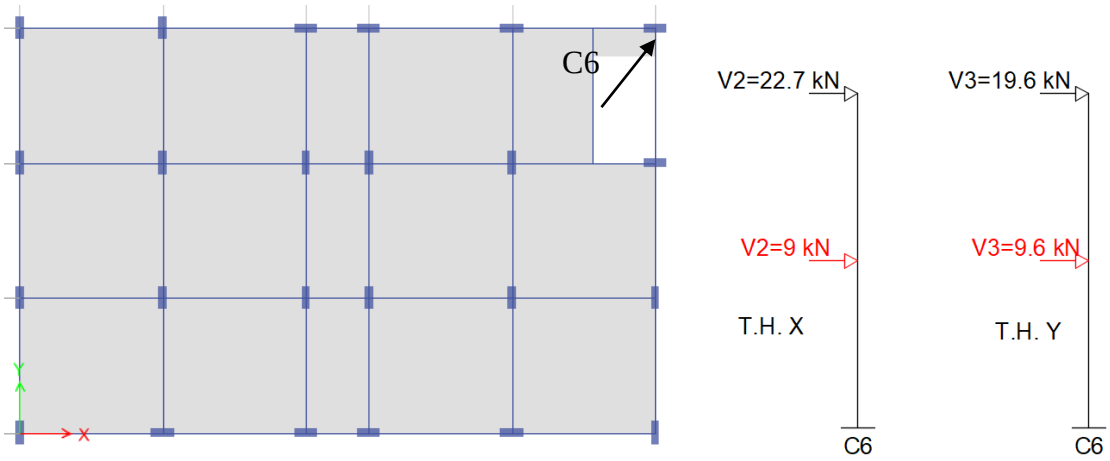

Figure 4.45: Column C6 shear forces under non-linear dynamic time history in both orthogonal directions.

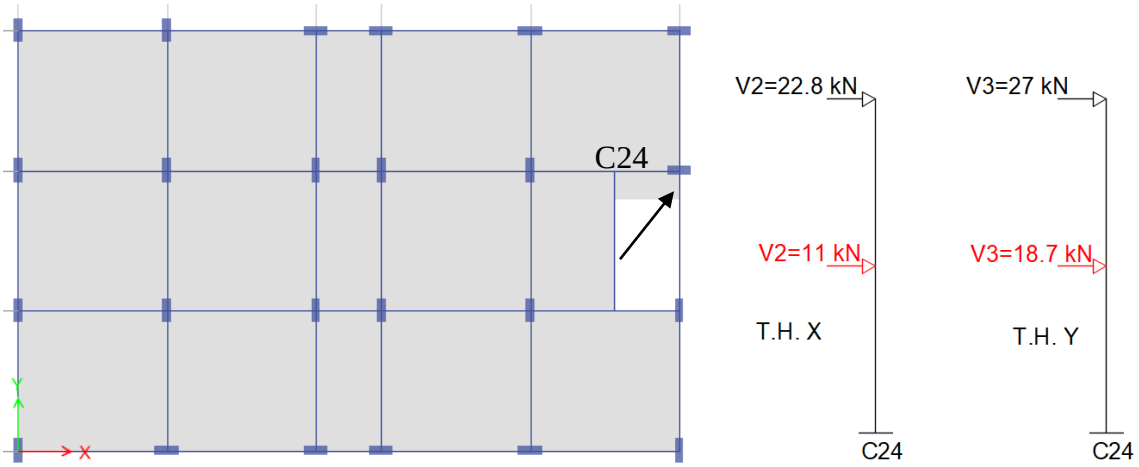

Figure 4.46: Column C24 shear forces under non-linear dynamic time history in both orthogonal directions.

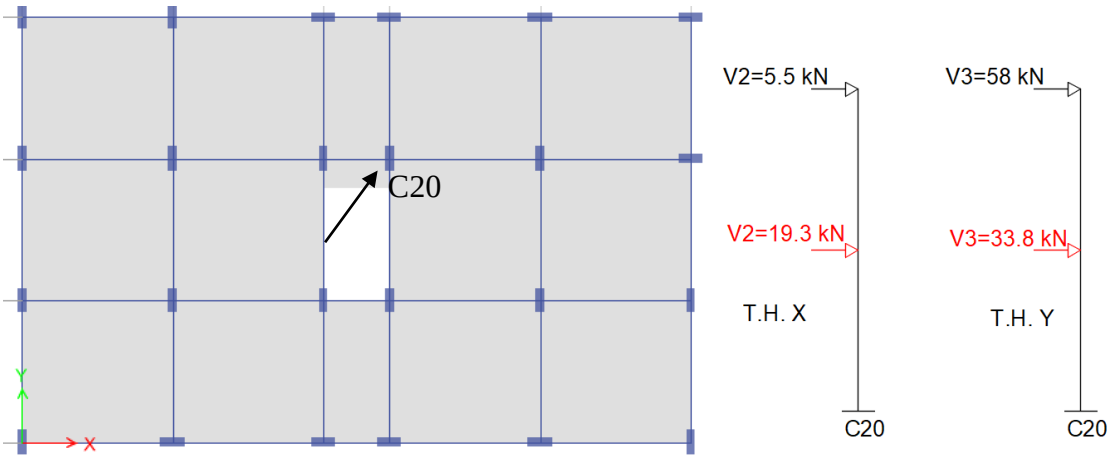

Figure 4.47: Column C20 shear forces under non-linear dynamic time history in both orthogonal directions.

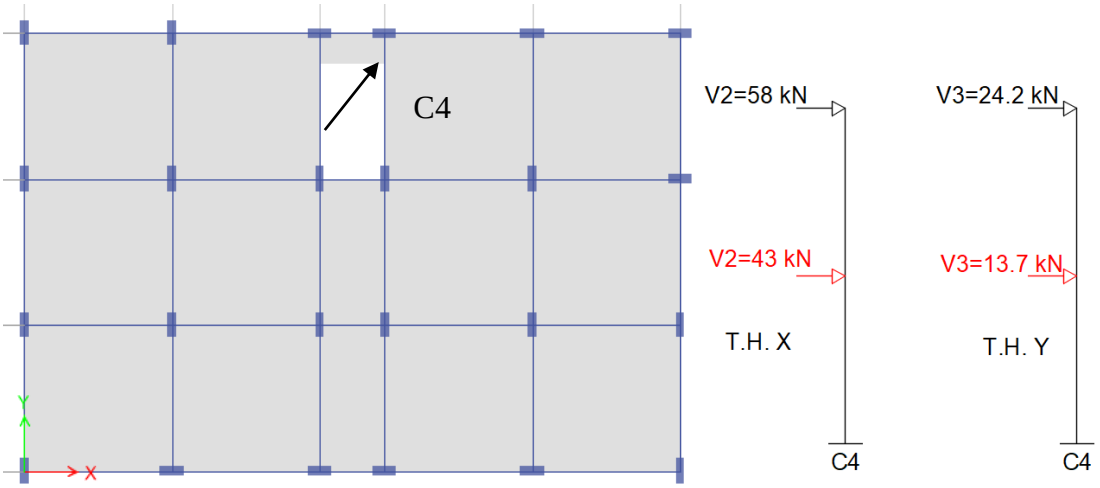

Figure 4.48: Column C4 shear forces under non-linear dynamic time history in both orthogonal directions.

The stirrups reinforcement must be adequate to resist the additional shear forces. To achieve an adequate resistance there are two suggestions, 1) the maximum allowable spacing distance between the stirrups bars should not be more than 10 cm, 2) the minimum allowable diameter of bars should be 10 mm in other words the confinement reinforcement zone of columns should be sufficient.

Chapter 5

CONCLUSION

5.1 Summary

The general description of models is eight reinforced concrete structures, four of them with staircase in four different locations and the other four without considering staircase. The structural system of the buildings is moment frame structure without any shear walls. The location of the building is supposed to be positioned in a highest-seismicity region of Turkey. Buildings are designed according to TS 500-2000 and Turkish Earthquake Code (2007), with considering seismic and gravity loads.

According to FEMA440, The Non-linear Static analysis has been clarified and utilized. The Non-linear Static analysis method is a comparatively simple method for evaluating seismic capacity and demand of reinforced concrete structures as explained in chapter 3. The method has been carried out by using CSI ETABS2016 program.

Time History analysis has been conducted. To perform Time History analysis three earthquakes have been considered which are Duzce earthquake, Kocaeli earthquake and Izmir earthquake. According to Turkish Earthquake Code the maximum results of the three considered earthquake is discussed. In this study the maximum results was in case of Duzce earthquake.

The main objectives of this study were to investigate the influence of the staircase presence and its location on the seismic performance of reinforced concrete building under lateral loads and dynamic loads in both orthogonal directions.

5.2 Conclusion

Based on the structural analysis by ETABS2016 software, major conclusions can be drawn from the present study are as follows:

Linear static analysis conclusion

- Torsional irregularity A1 occurred in all models that contain staircase. Inter-storey stiffness irregularity B2 was not formed in all models that involve staircase.
- Due to the staircase presence, the steel reinforcement ratios of staircase columns are increased significantly. It was found that the steel reinforcement ratios of columns that carry the landing slab of the staircase increased considerably in all models, while in columns that do not carry the landing slab there was slight effect.

Push over analysis conclusion

- It was observed that the presence and location of the staircase have an influence on the plastic hinges behaviour and their phases. The lowest number of collapse prevention plastic hinges was in model D that contain staircase and the highest number of collapse prevention plastic hinges in model A-1 that does not include staircase.
- It was obtained that the monitored and spectral displacements of all models (model A, B, C & D) that contain staircase were larger than the monitored

displacements of all models (model (A.1), (B.1), (C.1) & (D.1)) that do not involve staircase in both orthogonal directions.

- The base shear force was influenced by the staircase presence, however, the base shear force of all models (model A, B, C & D) that designed with considering staircase was significantly bigger than models (model (A.1), (B.1), (C.1) & (D.1)) that designed without considering staircase.
- It was found that the initial stiffness and effective stiffness of all models (model A, B, C & D) that contain staircase were greater than the initial stiffness and effective stiffness of all models (model (A.1), (B.1), (C.1) & (D.1)) that do not involve staircase in both orthogonal directions.

Time history analysis conclusion

- There was no significant difference in the diaphragm center of mass displacements of all models with and without staircase.
- The staircase presence and its location have not influence the max storey drift in all models with and without staircase.
- The formation of collapse prevention was affected by the staircase. The number of collapse prevention has decreased largely under non-linear dynamic load in Y direction comparing to the number under non-linear dynamic load in X direction.
- Model C that contain staircase in the middle of the structure had the minimum formation of collapse prevention when comparing with models that contain staircase.
- In columns which carry staircase landing slab there were an additional shear forces acting on the middle of the columns. This leads to create short columns

during earthquakes. In order to dissipate such a serious failures a sufficient confinement reinforcement region is necessary.

The staircases have importance influence on the seismic performance of RC buildings therefore the staircase shall be considered during modelling and designing structures. The structure frames that support staircase shall be reinforced properly to resist lateral forces during earthquake.

5.3 Recommendations

In this study only one type of reinforced concrete staircase in RC building has been considered.

- The same study is recommended for other type of reinforced concrete staircase.
- The same study is also recommended for reinforced concrete structures with shear walls.
- The same study is also recommended for steel staircase in RC buildings.

REFERENCES

Bechtoula, H., & Ousalem, H. (2005). The 21 May 2003 Zemmouri (Algeria) Earthquake: Damages and Disaster Responses. *Journal of Advanced Concrete Technology*, *3*(1), 161-174.

Code, T. E. (2007). Specification for structures to be built in disaster areas. *Ministry of Public Works and Settlement Government of Republic of Turkey*.

Council, B. S. S. (2000). Prestandard and commentary for the seismic rehabilitation of buildings. *Report FEMA-356, Washington, DC*.

Dai, H., & Qi, A. (2009). Analysis of performance of reinforced concrete frame structure with staircase based on ETABS [J]. *Journal of Earthquake Engineering and Engineering Vibration*, *6*, 016.

Dai, H. J., & Qi, A. (2010). Analysis on Seismic-response of Different Stiffness Reinforced Concrete Frame Structure with Staircase [J]. *Journal of Southwest University of Science and Technology*, *4*, 007.

Dai, H. J., & Qi, A. (2011). Analysis on seismic- response of reinforced concrete frame structure with different- thickness staircase. *Journal of Fuzhou University*, *39*(1), 101-109.

Inel, M., Ozmen, H. B., & Bilgin, H. (2008). Re-evaluation of building damage during recent earthquakes in Turkey. *Engineering Structures, 30(2)*, 412-427.

Jing, Y., Zhang, X., & Tina, Z. (2012). Elastoplastic response analysis of frame with slab stairs under severe earthquake. *World Earthquake Engineering, 1*, 011.

Ke, L. I., Fang-cun, S. O. N. G., Ke-shuan, M. A., & Jin-hua, X. I. A. (2011). Earthquake Impact Analysis for Stairs in Multi-storey Building on Whole Structure [J]. *Journal of Water Resources and Architectural Engineering, 5*, 013.

Li, B., & Mosalam, K. M. (2012). Seismic performance of reinforced-concrete stairways during the 2008 Wenchuan earthquake. *Journal of Performance of Constructed Facilities*, *27*(6), 721-730.

Roha, C., Axley, J. W., & Bertero, V. V. (1982). *The performance of stairways in earthquakes* (Vol. 82, No. 15). University of California, Earthquake Engineering Research Center.

Tapan, M., Comert, M., Demir, C., Sayan, Y., Orakcal, K., & Ilki, A. (2013). Failures of structures during the October 23, 2011 Tabanlı (Van) and November 9, 2011 Edremit (Van) earthquakes in Turkey. *Engineering Failure Analysis*, *34*, 606-628.

Turkish Standards Institute. TS500: Requirements for design and construction of reinforced concrete structures. Ankara. (Turkey); 2000.

Turkish Standard (1997), Design loads for buildings TS 498.

Sharma, K., Deng, L., & Noguez, C. C. (2016). Field investigation on the performance of building structures during the April 25, 2015, Gorkha earthquake in Nepal. *Engineering Structures*, *121*, 61-74.

Sun, H., Zhang, A., & Cao, J. (2013). Earthquake response analysis for stairs about frame structure. *Engineering Failure Analysis*, *33*, 490-496.

Zheng, J. J., Liao, Y. S., & Zhu, Y. P. (2011). Analysis and Calculation of Whole Frame Structure with Centre Staircase during Earthquake [J]. *Journal of Southwest University of Science and Technology*, *3*, 006.

ZHANG, R., ZHANG, X., & TIAN, Z. (2013). Research on the collaborate performance of board type stairs and frame in frequent earthquakes. *Sichuan Building Science*, *1*, 038.